RECONFIGURATION OF DISTRIBUTION NETWORK WITH DISTRIBUTED ENERGY RESOURCES FOR ENHANCING RESILIENCE.

by

Mohit P. Arora

A thesis submitted to the faculty of
The University of North Carolina at Charlotte
in partial fulfillment of the requirements
for the degree of Master of Science in
Engineering Management

Charlotte

2016

Approved by:

Dr. Churlzu Lim

Dr. Tao Hong

Dr. Badrul Chowdhury

Dr. Asis Nasipuri

ABSTRACT

MOHIT P. ARORA. Reconfiguration of distribution network with distributed energy resources for enhancing resilience.
(Under the direction of DR. CHURLZU LIM)

Enhancing the resiliency of the electric grid is a major challenge facing the electric regulatory bodies. Beyond the traditional approaches of improving the resiliency such as vegetation management, damage assessment and communication technology, the ever increasing share of Distributed Energy Resources (DER) can be used as a way of modernizing the grid. Strategically placed DER's can be effectively used to reduce the vulnerability of the interconnected system and also, reduce customer outage time. Although connecting the DERs into the traditional electric network can pose technical and regulatory challenges, they can be used efficiently to form smaller standalone grids or micro-grids during hours of emergency and extreme weather scenarios. In this study, we propose a modernized approach for optimally supplying loads using mixed integer linear programming (MILP) under multiple power outages by maximizing the loads assigned to each node. The scope of the problem is further expanded to form a MILP formulation for a three phase electric network taking into account the power balance and operational constraints. A numerical example with a real system is used to illustrate the effectiveness of both the formulations.

DEDICATION

To my parents, my advisor and my friends for being a great source of support throughout this journey.

ACKNOWLEDGEMENTS

I would like to begin by thanking my advisor, Dr. Churlzu Lim, for his constant guidance and motivation. Dr. Badrul Chowdhury for providing the technical insight on the problem at hand. Together their key inputs helped steer this research work towards its goal. I would also like to thank Dr. Asis Nasipuri and Dr. Kalpathi R. Subramanian, for their advice on the research. I'm grateful to the individuals at Duke Energy for taking time out of their busy schedules and providing the network data. Especially, Mr. Andrew Kling for his invaluable input during the weekly meeting and providing access to the different network data. I would also like to thank the Systems Engineering and Engineering Management Department, College of Engineering and Mosaic Computing for providing access to AMPL and other computing facilities. I am grateful to Mr. Md. Shakawat Hossan and Mr. Christopher Grafer, for providing their help in cleansing and manipulating of the grid data and visualization of results.

TABLE OF CONTENTS

LIST OF FIGURES

LIST OF TABLES

CHAPTER 1: INTRODUCTION

The U.S. Electricity network is one of the largest and complex engineering achievement of the 20^{th} century. With the rapid development of the economy, the domestic, industrial and commercial demands for electricity have increased tremendously. The problems on the traditional electric system have intensified with the ever changing customer needs and advancements in smart grid and communication technologies [1].

Recent natural events such as Hurricane Sandy and Katrina have caused severe power outages and raised the question about the sustainability of the network against such extreme natural disasters. Hurricane Sandy left 7.5 million customers without power across 15 states and Washington, D.C. [2]. Even days after the event, millions of customers were left without power throughout the East Coast, which incurred billions of dollars in damages. An analysis by Lawrence Berkeley National Laboratory's Evan Mills shows that approximately 78% of the 1,333 gird outages in the period of 1992 to 2010 were weather related and affected 178 million customers in the U.S. alone [5]. The economic cost of power outages is largely related to the duration of the outage. In 2001, EPRI estimated that the annual cost of weather related outages is about $104 billion to $164 billion, with about 44% to 78% being weather related outages. The total estimated economic loss can be estimated from $20 billion to $70 billion per year [5]. In the recent years, with the increasing number of weather related outages these numbers would be even higher. The aging electric grid and ever increasing power demand have highlighted the need for a reliable and resilient power delivery infrastructure [2].

The Department of Energy and electric utilities have taken certain traditional measures such as vegetation management, damage assessment, and communication technology, and backup generators, etc. to decrease the vulnerability of the system against natural attacks. A detailed explanation on the measures that can be adopted to enhance the resiliency is given in [4] and [5]. Recently, there has been extensive research on small independently islanded grids, called as *micro-grids*, which operate as a standalone feeder system.

Distributed Energy Resources (DERs) have gained commercial importance recently. DERs may include photovoltaic systems (solar cells), energy storage devices, wind systems, and fuel cells. In spite of their high installation costs, DERs are proven to be cost effective in the long run. Many commercial building, industrial warehouses and distribution centers have installed solar panels to satisfy their energy needs. When combined with storage devices, surplus energy generated by these solar panels can be stored, and used during other times of the day when sufficient solar energy is not available. This additional energy can also be used to satisfy the needs of the neighboring loads and form small micro-grids. For example, retail giant Walmart has about 180 revenewable energy initiatives which generate 89 megawatts (MW) as reported by the Solar Energy Industries Association [3]. Figure 1.1 shows the Walmart's distribution center in Buckeye, Arizona, which has a total of 14,000 roof and car parking canopy solar panels and produces solar energy enough to fulfill 30% of its demand. [3].

In situations where the load points are disconnected from the main feeder and/or where multiple line outages occur in the network, strategically placed and connected DERs have potential to be utilized in order to supply electricity to the disconnected areas by forming small micro-grids. DERs can temporarily supply the loads until when the line outages are fixed and the main feeder can supply power. The micro-grids formed by the DERs can operate in an island mode, where the load points connected in the micro-grid are supplied locally by the DERs and also in a grid connected mode where the loads are powered by the feeder system and DER together. Although there

Figure 1.1: Walmarts distribution center at Buckeye, Arizona

Source: Hower, M.(2013, October 30) Walmart Now Produces More Solar Power Than 38 U.S. States. Retrieved April 07, 2016, from *http://www.sustainablebrands.com/news_and_views/clean_tech/mike-hower/walmart-now-produces-more-solar-power-38-us-states*

are certain operational concerns regarding the switching capabilities and monitoring of DERs to supply power into the conventional distribution network, DERs have great potential to be effectively used in times of emergency or extreme weather events to supply electricity to the disconnected loads.

During crisis, critical facilities such as hospitals, schools, fire stations, police stations, etc. have to be given higher priority over domestic and commercial loads, especially when there is insufficient power from DERs to cover all outage areas. Besides, determining the loads to be supplied during emergency needs to take the operational and connectivity constraints into consideration, which results in a complex decision making process. Mathematical optimization can beneficially be employed to make such a complex decision. The formulation proposed in this study is a Mixed Integer Programming (MIP) problem which maximizes the total priorities assigned to each load in the network. Initially, the formulation was developed for a single phase radial network, later it is extended to consider a 3-Phase radial network and to incorporate nonlinear power balance equations. The proposed formulation aims to tackle the issues of dynamic network reconfiguration by using the DERs to form micro-grids and also the supply of critical facilities during weather related outages. An example of a real utility feeder system is used to determine the effectiveness of the both the formulations and results are presented.

The rest of the thesis is organized as follows. Chapter 2 provides a thorough literature review on the previous research about strategies for coping with power outages, using DERs during emergency and optimization models. Chapter 3 describes the details of the mathematical formulation for the single phase radial network. Chapter 4 presents an extended mathematical formulation for the three phase radial network. Chapter 5 provides further extension to by incorporating nonlinear power flow balance equations and converting a meshed non-radial network to a radial distribution network. Chapter 6 presents the numerical results for the proposed formulations by using a real distribution network with fault scenarios. The conclusion and future direction of the research is given in Chapter 7.

CHAPTER 2: LITERATURE REVIEW

In this chapter, we provide a review on the previous research in the utilization of optimization techniques for enhancing the resiliency of the distribution networks and preliminaries to basic mixed integer programming formulations.

2.1 Literature Review on Resiliency of Distribution Network

When a major fault occurs in a distribution network, the primary goal of the utility operators is to restore the power system as quick as possible. The first step involves detecting the fault and identifying the location and the second step is to restore power to as many customers as possible. With the help of automated switches located in the grid, utility operators can remotely redirect the power through the healthy lines by a sequence of controlled switching operations [6].

There has been extensive research in the literature on system restoration after a fault by changing the network configuration by switching operations to reduce the restoration time. *Liu et al.* [7] propose an expert system which contains a knowledge base of 180 rules which can be used by utility operators to restore power to maximum number of load zones. *Chen, Lin and Tsai* [8] also propose a rule-based expert system along with a colored Petri Net (CPN) model where priority indices are assigned to each zone and feeder for identifying important load points for prioritized service restoration. The effectiveness of the model is shown using an 18 feeder distribution system of Taiwan Power Company. A use of two step fuzzy logic methodology has also been proposed in [9] and [10] for service restoration for a single fault and multiple faults, respectively. Multi-agent solution has also been proposed for service restoration in *Solanki et al.* [11], where the objective is to maximize the power satisfying loads with weights assigned to them. A heuristics search using a binary depth first search (DFS) tree algorithm has been also proposed, so that operators can be guided to narrow the search and find the best possible switching decision for service restoration in the smallest amount of time [12].

Optimization has also been used for system restoration. *Khushalani et al.* [13] also propose a mixed integer nonlinear programming problem for system restoration after a fault. They consider an unbalanced three phase feeder system for which they propose two formulations. In the first problem, they consider the objective of maximizing the two priority levels (vital and semi-vital) assigned to the nodes along with the switching and three phase system constraints. Due to the nonlinear nature of the formulation, a problem with small number of nodes can be solved but for larger number it fails to converge. Next, to tackle this issue, they consider a multi objective function which aims to maximize the power in the network while minimizing the number of switching operations required. They demonstrated the effectiveness of the formulation by finding the global optimal solution for two modified IEEE test distribution systems. Other methods such as artificial neural networks [14], genetic algorithms [15], and hybrid optimization models [16] have also been proposed in literature for the network restoration and reconfiguration [17]. *Nyugen, and Flueck* [17] consider a multi agent based model where they consider two types of agents: switching agents and distribution energy storage (DES) agents to form micro-grids after faults in the distribution system.

There has been tremendous research in reconfiguration and restoration techniques after faults in the distribution network as seen above. In extreme weather events, we need to consider the worst possible scenarios such as multiple faults in the distribution system and/or the sub-station is disconnected from all/majority of the distribution network and/or the neighboring feeder systems cannot be reconfigured to supply the faulty feeder system. DERs scattered throughout the system network can be used advantagiously to supply power to the critical customers under these conditions. Initially, DERs existed in the form of back-up generator which were able to restore power to the customers in the load bus it was connected in case of an interruption [18]. But, DERs were not able to supply power to the nearby load busses. With the increasing advancements in communication technologies and automated switching devices, the new generation of DERs such as solar PV, small hydro, wind-turbines, etc. can be used to restore load beyond its own load to the nearby critical loads to form a micro-grid. The location of the faults during a disastrous events are unknown. Therefore, formation of micro-grids for DERs should be dynamic after the fault location has been identified [19].

There has been an increasing interest in literature for utilization of DERs in restoration of the distribution system after faults. *Pham et al.* [20] propose a knapsack combinatorial optimization model for DER after a major fault. Its objective is to maximize the power that is supplied to nodes based on their weighted priorities. They consider finding the optimal switching sequence for a single DER with black-start capability in a network by using the branch and bound algorithm. A multi agent based algorithm is proposed for load restoration by forming micro-grids in *Xu and Liu* [21], they consider each bus in the micro-grid as an agent which communicates with the neighboring nodes to form the optimal micro-grid. The knapsack optimization model is proposed to find the optimal decision for the nodes to be supplied by the DER. Knapsack problems are NP-hard and the global optimal solution is hard to achieve where time availability is limit. *Castillo* [22] considers a multi-stage stochastic MILP model for restoration of power and damage assessment after a natural disaster for pre-installed micro-grids. The aim of the formulation is to reduce the restoration time considering the power flow operations and optimal scheduling over the timespan of the fault. A multi-objective nonlinear optimization problem is considered in *Li et al.* [23] which considers minimizing the switching operations while maximizing the total load restored in the distribution system along with static voltage and current operational constraints to check for violations. They consider modelling the micro-grids as virtual feeders in the network and use the spanning search tree to find the optimal load busses to be restored. The distribution system restoration (DSR) algorithm proposed in [23], has only been tested for single fault and does not consider multiple faults scenario, which may arise during severe weather events. Similarly, other methods such as stochastic models [24], and control algorithms [25] have been proposed for utilization of DERs and micro-grids in system restoration after a fault.

Recently, *Chen et al.* [19] developed a MILP problem forming dynamic micro-grid after multiple faults occur in the network. They propose a formulation for maximizing the weight priorities for all the nodes picked by the DERs in the dynamic micro-grid formation for a single phase network. They consider the topological, switching and linearized power balance constraints when selecting the nodes that can be picked by a DER for its micro-grid. They propose a de-centralized multi-agent coordinated information system in which multiple local agents coordinate and communicate information with the regional agents which solve the MILP problem for formation of micro-grids. However, developing such a communication requires advanced communication devices which are costly to implement in the field. In this study, we propose a single phase and three phase systems which can be easily implemented and incorporated within the utilities Supervisory Control And Data Acquisition (SCADA) systems.

We assume the DERs are disconnected from the main distribution system under normal operations. In case of multiple faults, each DER can be connected to the main distribution network in order to form its own micro-grid by connecting to nearby nodes. The system is assumed to have communication capabilities to identify and isolate the faulty region. The formulations proposed here form dynamic micro-grids in the distribution network for each DER considering multiple fault isolations in the network.

2.2 Background on Mixed Integer Programming (MIP)

Linear programming (LP) was first introduced by George Dantzig in 1947. Subsequently, many scientists have made many significant contributions to the topic [26]. Linear programming has been used extensively in government and industries such as defense, logistics, manufacturing, financial services, telecommunications, retail, etc. [27]. Linear programs consider the objective of the problem and their conditions to be linear. Many of the large scale optimization problems are modelled as linear programs because of their simplicity, ease of understanding and global optimal solutions are usually guaranteed. Integer linear programs have variables restricted to take only integer values. Binary variable which only take the value of $[0, 1]$, are also considered as integer variables. An integer linear program in its standard form can be expressed as [28],

$$\text{Maximize} \quad \sum_{j=1}^{n} c_j x_j \tag{2.1}$$

$$\text{Subject to,} \quad \sum_{j=1}^{n} a_{ij} x_j = b_i \qquad (j = 1, 2, ..., m) \tag{2.2}$$

$$x_j \geq 0 \qquad (i = 1, 2, ..., n) \tag{2.3}$$

$$x_j \ \textit{integer} \qquad (\textit{for some or all } j = 1, 2, ..., n) \tag{2.4}$$

Equation 2.1 represents the linear objective function, where c_j is the constant parameter and x_j is a integer variable, where j represents the index of the variable in vector consisting n. The aim of the objective is to *maximize* or *minimize* the objective function value. In the equation 2.2, a_{ij} and b_i represent constraint coefficient parameters and constant right hand side parameters, respectively. Equation 2.3 represents the lower bound on all the variables. This constraints can be sometimes replaced by, $l_j \leq x_j \leq u_j$, where l_j and u_j are the lower and upper bounds for the variable x_j, respectively. Equation 2.4 represents the constraint for declaring that some or all the variables are integer valued, including binary.

If all the variables in the formulation are declared as integer, it is called a pure integer linear program. If some variable are integer and others are continuous, the program is considered as a mixed integer linear program (MILP). The two formulations proposed here in Chapter 3 and 4 are MILPs. We propose a mixed integer nonlinear program (MINLP) in Chapter 5, which is an extension of the MILP formulation in Chapter 3 by incorporating nonlinear power balance equations into the constraint set.

CHAPTER 3: SINGLE PHASE MATHEMATICAL FORMULATION

In this chapter, the single phase formulation for a radial network is explained in detail. Consider an electric network that consists of nodes and links. Suppose that DERs are placed at nodes and can be remotely controlled to be connected or disconnected from the network. We also assume that the DERs can generate enough power to satisfy its own energy demand and also supply neighboring load points in the network. Hence, in case of a fault on the main line or lateral, the surplus power available at the DER can be used as a source to satisfy the demand of the neighboring load points and can form a self-satisfying micro-grid in the network.

We assume that exact fault location can be identified by sensor (e.g. wireless sensor network) and can be communicated to main Supervisory Control and Data Acquisition (SCADA) system. Hence, the information about the power outage area, such as healthy lines and available power at DERs is readily available for the proposed optimization model to be employed. Distribution network typically contain only a limited number of reclosers or additional switching equipments. However, due to advanced technology, more affordable switching devices will emerge in the near future. Hence, we assume that such switching devices are available in the network.

The problem is first represented by a radial network which consists of a set of nodes N and the distributed energy resources in the network are represent by set K, where $K \subset N$. The nodes of the network are connected by directed edges, represented by $E(i, j, k)$, where $(i, j) \in N, k \in K$. Note that edges are layered over $k \in K$, so that power flows can be made in different directions depending on the DER that supplies the power. The formulation proposed here is similar to the one proposed in [19] with exception of some switching constraints and the objective.

3.1 Objective Function

The proposed MILP is formulated such that the objective function aims at maximizing the weighted sum of nodes that can be supplied by the available DERs in the network, where weights are assigned to each and represent priorities. Let, w_i denote the weight assigned to node i, $i \in N$. While weights can take on general values, they can be discretized for the sake of practicality. For example in our numerical example, the weights have been categorized into three levels. Load points such as Hospitals, Fire Stations, Police Stations, etc. have been given the highest priority with a weight of 1000. The second priority has been given to residential and other commercial loads with a weight of 100. The last category are the points carrying no loads and are just forwarding the power, which have been assigned a weight of 0. Define, binary variable y_i is used to determine if a node i is being supplied in the network.

$$y_i = \begin{cases} 1 & \text{if node } i \text{ is connected,} \\ 0 & \text{otherwise} \end{cases} \qquad i \in N$$

Then, the objective function is the summation of the product of the weights and the nodes being supplied in the network. The objective function can be represented as

$$\text{Maximize} \qquad \sum_{i \neq k} w_i y_i \tag{3.1}$$

3.2 Constraints

3.2.1 Connectivity Constraints

If a node is connected, it can be connected to only one DER in the network. A binary variable x_{ik} is defined to determine if node i is connected to DER k in the distribution network for $i \in N, k \in K$. The binary variable $x_{ik} = 1$, if node i is connected to DER k in the network and $x_{ik} = 0$, otherwise.

$$\sum_{k \in K} x_{ik} \leq 1 \qquad i \in N/K \quad (3.2)$$

Assume, that the node where a DER is located, is connected to the same DER. This constraint can be represented as,

$$x_{kk} = 1 \qquad k \in K \quad (3.3)$$

The next constraint assure that there exists a path to a node from DER k, if DER

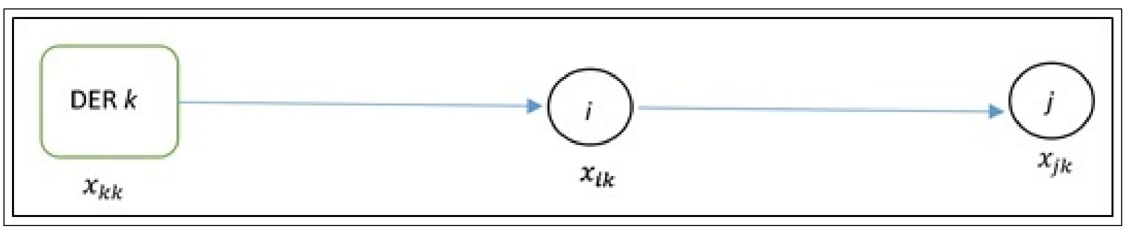

Figure 3.1: Connectivity of from-node to to-node in relation to DER

k supplies to this node. From 3.1 it can be seen that, If node j is supplied by DER k, then node i, the parent node of j must also be supplied by the same DER k for each directed edge $(i, j, k) \in E$, where $(i, j) \in N$ and $k \in K$. In other words, if the from-node i is not connected to DER k, then the to-node j cannot be connected to DER k.

$$x_{jk} \leq x_{ik} \qquad (i, j, k) \in E \quad (3.4)$$

3.2.2 Relationship between x and y

The binary variable x_{ik} can be related to the binary variable y_i using the constraint,

$$y_i = \sum_{k \in K} x_{ik} \qquad i \in N/K \quad (3.5)$$

From equation 3.2, it can be seen that node i can only be connected to up to one DER k. So, $y_i = 1$ if the node i is connected in the network and $y_i = 0$, if the node is not connected in the network.

3.2.3 Fault Identification Constraint

A set F is defined to indicate all the faulty nodes in the network, where $F \subset N$. The faulty nodes identified should not be connected in the network. This can be achieved by forcing $y_i = 0$. This forces the faulty node i not to be connected in the network, thus excluding it from the network. This constraint also forces the binary variable $x_{ik} = 0$, in equation 3.5, therefore not connecting it to any DER. The fault identification constraint can be represented as,

$$y_i = 0 \qquad i \in F \quad (3.6)$$

3.2.4 Linearized Power Balance Constraints

The nodes connected to a DER, should also satisfy the power flow constraints. Power flow constraints are often approximated by a linearized form. In this research, the DistFlow Model from [29] and the linearized version of the equations are taken from [30]. The variable P_{ik} is defined to represent the real power flow into the node i from DER k. For each $k \in K$, the real power balance constraint can be formulated as the total sum of the power originated from DER k and sent to forward star of node i ($FS(i)$) is equal to the power delivered to node i from DER k minus the power consumed at node i. From Figure 3.2, it can be seen that nodes $j1$ and $j2$ are the forward star of node i. The sum of the real and reactive power directed towards nodes $j1$ and $j2$ should be equal to the real and reactive power remaining at node node i after its own real and reactive demand is served, respectively.

$$\sum_{j \in FS(i)} P_{jk} = P_{ik} - p_i x_{ik} \qquad i \in N, k \in K, \quad (3.7)$$

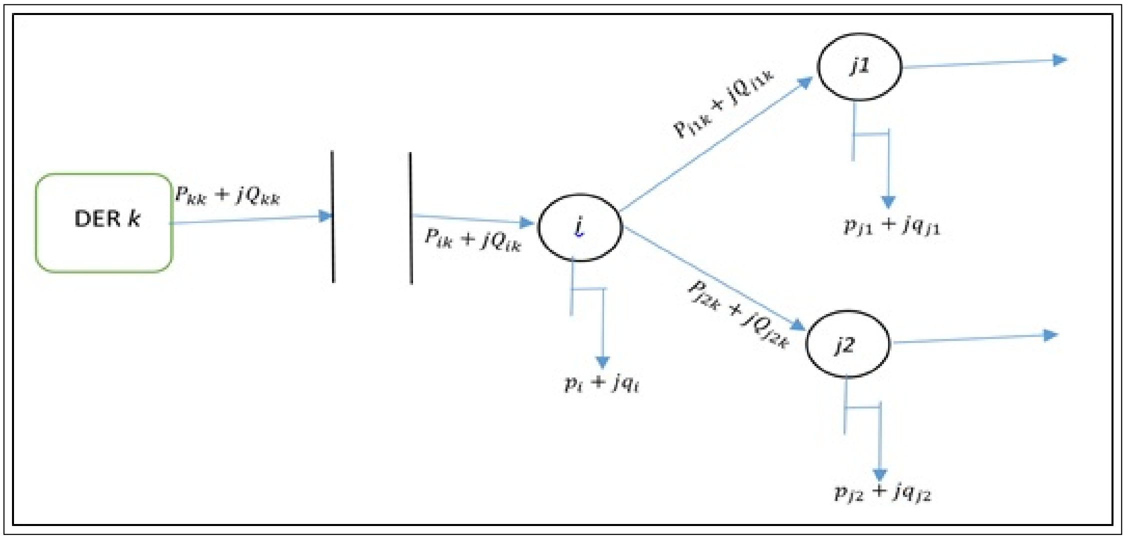

Figure 3.2: Real and reactive power balance among nodes

where p_i = real power demand at node i $\qquad i \in N$

Similarly for reactive power, define variable Q_{ik} as the reactive power flow into node i from DER k and the reactive balance constraint can be written as

$$\sum_{j \in FS(i)} Q_{jk} = Q_{ik} - q_i x_{ik} \qquad i \in N, k \in K, \quad (3.8)$$

where q_i = reactive power demand at node i $\qquad i \in N$

From constraints 3.7 and 3.8, it can be seen that the real demand for only those nodes connected to DER k would be considered, i.e., if $x_{ik} = 1$, then p_i and q_i will be subtracted from the real power (P_{ik}) and reactive power (Q_{ik}) that node i receives, and the remaining real and reactive power would be passed on to forward star of node i, respectively. Note that, if there is no power demand at node i, then the entire power flowing into node i will be passed on to the forward star of node i. If node i is not connected to DER k, then the real and reactive power flow into node i from DER k

must be zero. To enforce this, the following constraints are used.

$$0 \le P_{ik} \le P_k x_{ik} \qquad i \in N, k \in K \quad (3.9)$$

$$0 \le Q_{ik} \le Q_k x_{ik} \qquad i \in N, k \in K, \quad (3.10)$$

where P_k = real capacity at DER k $\qquad k \in K$

Q_k = reactive capacity at DER k $\qquad k \in K$

These constraints force the real and reactive power flows into node i to be zeros, if the node i is not connected to DER k, i.e., if $x_{ik} = 0$, then P_{ik} and Q_{ik} are forced to be zeros. For the nodes connected to DER k, i.e., $x_{ik} = 1$, then P_{ik} and Q_{ik} should be less than or equal to the capacities of the DER k. For the nodes where DERs are installed, i.e., $i = k$, the binary x_{ik} is always equal to 1. Therefore for the DER nodes, the above constraints 3.9 and 3.10, the real power (P_{ik}) and reactive power (Q_{ik}) are less than or equal to the real and reactive capacities of the DER k, respectively.

3.2.5 Voltage Constraints

The voltage constraints mentioned below are a part of the power balance and operational constraints. For ease of presentation, they have been explained in a different sub-section. The linearized voltage equation from the DistFlow Model [30] has been modified into an inequality constraint to suit the problem. Due to the impedance of lines, voltage drops when the power flows on the line. To enforce the voltage drop, variable V_{ik} represent the voltage at node i connected to DER k. The voltage at the DER nodes is denoted by V_{kk} which is a constant voltage and is defined by constant ν. For example, in our numerical example, a value of 7.2 kV is assigned for all DERs for the entire network considered. This value can be different for different networks.

The linearized voltage constraints for an edge $(i, j, k) \in E$ are

$$V_{jk} \leq V_{ik} - \frac{r_{ijk} P_{ik} + s_{ijk} Q_{ik}}{RV_k} \qquad (i, j, k) \in E \quad (3.11)$$

$$V_{kk} = \nu \qquad k \in K, \quad (3.12)$$

where r_{ijk} = resistance in line *(i,j)* $\qquad (i, j) \in N, k \in K$

s_{ijk} = reactance in line *(i,j)* $\qquad (i, j) \in N, k \in K$

RV_k = reference voltage for DER k $\qquad k \in K$

Similar to the constraints 3.9 and 3.10 for real and reactive power, the voltage V_{ik} should be zero if the node i is not connected to DER k. If node i is connected to DER k, the voltage at node i is limited by an upper bound. This constraint can be expressed as,

$$0 \leq V_{ik} \leq RV_k x_{ik} \qquad i \in N, k \in K \quad (3.13)$$

The last constraint is to enforce voltages to be within acceptable range, which a determined by the tolerance limit of the nominal voltage of the network. Hence, for each node V_{ik} must remain between the upper tolerance and the lower tolerance limits of the nominal voltage.

$$(NV(1 - t))x_{ik} \leq V_{ik} \leq (NV(1 - t))x_{ik} \qquad i \in N/K, k \in K, \quad (3.14)$$

where NV = nominal voltage of the network

t = voltage tolerance limit of the network

3.3 Notations

3.3.1 Variables

$$y_i = \begin{cases} 1 & \text{if node } i \text{ is connected,} \\ 0 & \text{otherwise} \end{cases} \qquad i \in N$$

$$x_{ik} = \begin{cases} 1 & \text{if node } i \text{ is connected to DER } k, \\ 0 & \text{otherwise} \end{cases} \qquad i \in N, k \in K$$

$$P_{ik} = \text{real power flow into node } i \text{ from DER } k \qquad i \in N, k \in K$$

$$Q_{ik} = \text{reactive power flow into node } i \text{ from DER } k \qquad i \in N, k \in K$$

$$V_{ik} = \text{voltage at node } i \text{ from DER } k \qquad i \in N, k \in K$$

3.3.2 Parameters

w_i = weight assigned to node i	$i \in N$
p_i = real power demand at node i	$i \in N$
q_i = reactive power demand at node i	$i \in N$
P_k = real capacity at DER k	$k \in K$
Q_k = reactive capacity at DER k	$k \in K$
r_{ijk} = resistance in line *(i,j)*	$(i, j) \in N, k \in K$
s_{ijk} = reactance in line *(i,j)*	$(i, j) \in N, k \in K$
RV_k = reference voltage for DER k	$k \in K$
ν = Initial voltage at the DER	
NV = nominal voltage of the network	
t = voltage tolerance limit of the network	

3.4 Formulation

In summary, the mixed integer linear programming formulation is as follows.

$$\text{Maximize} \quad \sum_{i \neq k} w_i y_i$$

subject to,

$$\sum_{k \in K} x_{ik} \leq 1 \qquad i \in N/K$$

$$x_{kk} = 1 \qquad k \in K$$

$$x_{jk} \leq x_{ik} \qquad (i, j, k) \in E$$

$$y_i = \sum_{k \in K} x_{ik} \qquad i \in N/K$$

$$y_i = 0 \qquad i \in F$$

$$\sum_{j \in FS(i)} P_{jk} = P_{ik} - p_i x_{ik} \qquad i \in N, k \in K$$

$$0 \leq P_{ik} \leq P_k x_{ik} \qquad i \in N, k \in K$$

$$\sum_{j \in FS(i)} Q_{jk} = Q_{ik} - q_i x_{ik} \qquad i \in N, k \in K$$

$$0 \leq Q_{ik} \leq Q_k x_{ik} \qquad i \in N, k \in K$$

$$V_{jk} \leq V_{ik} - \frac{r_{ijk} P_{ik} + s_{ijk} Q_{ik}}{RV_k} \qquad (i, j, k) \in E$$

$$V_{kk} = \nu \qquad k \in K$$

$$0 \leq V_{ik} \leq RV_k x_{ik} \qquad i \in N, k \in K$$

$$(NV(1-t))x_{ik} \leq V_{ik} \leq (NV(1-t))x_{ik} \qquad i \in N/K, k \in K$$

CHAPTER 4: THREE PHASE MATHEMATICAL FORMULATION

In this chapter, the formulation from Chapter 3 is extended to accommodate a three phase unbalanced radial network. Distribution systems for utilities are generally three phase unbalanced networks. The mathematical formulation proposed in this chapter for a three phase unbalanced radial network can effectively represent the distribution systems in the real world. The solution obtained from the optimization model will identify the load points and corresponding power flows on different phases from different DERs.

Suppose that the distribution network is connected by three phases, a, b and c. Accordingly, in addition to the assumptions mentioned in Chapter 3 it is assumed that the DERs can be connected in a single phase, two phases or all three phases via any one of the following combinations: a, b, c, ab, bc, ac, and abc. While the load at the node is known, the power to be supplied by the DER in each phase is unknown when the node is connected in multiple phases.

Furthermore, a load point can be connected to one DER in each phase but it can be connected to different DER in different phase. For example, if a load point is connected in two phases, e.g. ac, the load point can be connected to a DER in phase a and another DER in phase c. For this problem, we do not consider partial fulfillment of load demand at a node. For example, if a load point is connected in all three phases abc, the total power that the node receives via a, b and c must be same as the power demand at the node. In other words, if the entire demand cannot be supplied, the node should not be connected.

Consider, a radial network that has the load points in a set of nodes N. The three phases in the network are represented by a set $\Phi = (a, b, c)$. The DERs in the network are denoted by set K, where $K \subset N$. The directed edges for each phase and for each DER in the distribution network are represent by (i, j, ϕ, k), where $(i, j) \in N$,$\phi \in \Phi(j)$ and $k \in K$.

4.1 Objective

The objective function for this problem is same as the one in chapter 3. That is, the objective function aims at maximizing the weighted sum of nodes supplied by the DERs, where weights represent priorities of nodes. Accordingly, w_i denotes the weight assigned to node i where, $i \in N$. The binary variable y_i indicates the connectivity of node i, such that

$$\text{Maximize} \qquad \sum_{i \neq k} w_i y_i \tag{4.1}$$

4.2 Constraints

4.2.1 Phase Connectivity Constraints

In each phase, a node i can only be connected to one DER in the network. The binary variable $x_{i\phi k}$ indicates whether the node is connected in each phase. The variable $x_{i\phi k} = 1$, if node i is connected to DER k in phase ϕ and $x_{i\phi k} = 0$, if the node is not connected.

$$x_{i\phi k} = \begin{cases} 1 & \text{if node } i \text{ is connected in phase } \phi \text{ to DER } k, \\ 0 & \text{otherwise} \end{cases} \qquad i \in N, \phi \in \Phi(i), k \in K$$

At each node, one phase can be connected to at most one DER.

$$\sum_{k \in K} x_{i\phi k} \leq 1 \qquad i \in N/K, \phi \in \Phi(i) \quad (4.2)$$

The nodes where a DER is located, should always be connected to the same DER in the phases it is connected. Let $\Phi(i) \subset \Phi$, be the set of phases node i is connected in. Then, we have

$$x_{k\phi k} = 1 \qquad \phi \in \Phi(k), k \in K \quad (4.3)$$

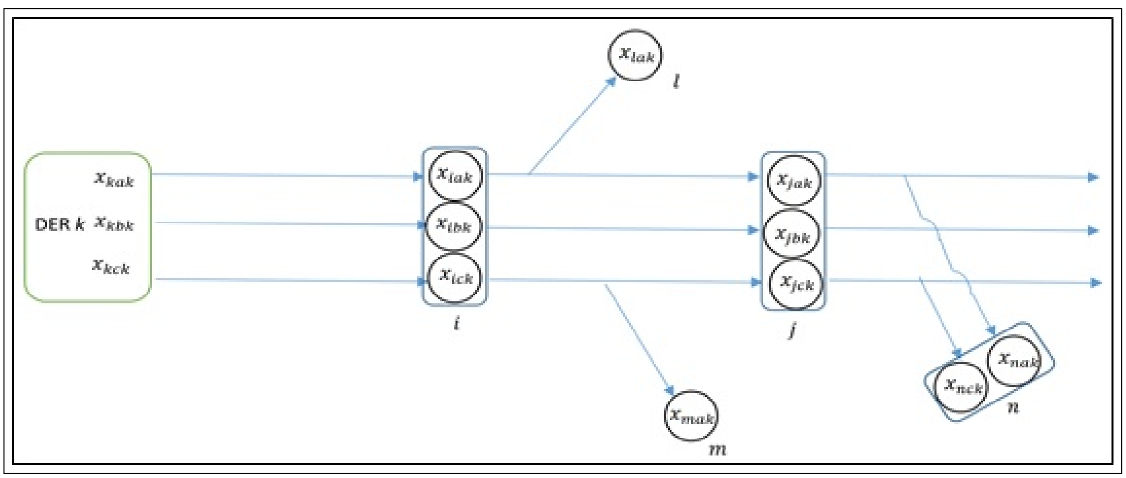

Figure 4.1: Connectivity of from-node and to-node in relation to DER and phase

For each directed arc (i, j, ϕ, k) in set E, if node j is supplied by DER k in phase ϕ , the node i should also be supplied by DER k in phase ϕ . Figure 4.1 illustrates a network representation of this constraint. This constraint can be expressed as,

$$x_{j\phi k} \leq x_{i\phi k} \qquad (i, j, \phi, k) \in E \quad (4.4)$$

4.2.2 Relationship between x and y

The phase specific $x_{i\phi k}$ for node i can be related to the binary variable y_i as follows. Let h_i denote the cardinality of $\Phi(i)$, i.e., $h_i = |\Phi(i)|$. $h_i = 1$, if node i is connected in single phase, $h_i = 2$ if the node is connected in any combination of the two phases $(ab, bcorac)$ and $h_i = 3$ if the node is connected in all the three phases, abc.

$$\sum_{k \in K} \sum_{\phi \in \Phi(i)} x_{i\phi k} = h_i y_i \qquad i \in N/K \quad (4.5)$$

Note that this constraint assumes that, if a node is connected, all phases associated with the node must be connected.

4.2.3 Fault Identification Constraint

The fault identification is the same as used in Chapter 3 equation 3.6. For any node belong to the faulty nodes set F, the node should not be connected to the network in all the phases. This is accomplished by setting $y_i = 0$ for all $i \in F$. Then, the node i will not be connected in any phase in the network. The constraint is expressed as,

$$y_i = 0 \qquad i \in F \quad (4.6)$$

4.2.4 Phase Power Balance Constraints

The equations from linearized power balance constraints in Chapter 3 are extended to accommodate a three phase distribution network. Recall that the overall real and reactive powers at the load point are known. Define variables to represent real and reactive demand in each phase ϕ at node i using $p_{i\phi}$ and $q_{i\phi}$ respectively, for $i \in N, \phi \in \Phi(i)$. The overall real and reactive demands at node i is denoted by PD_i and QD_i, for $i \in N$. $P_{i\phi k}$ denotes the real power flow into node i in phase ϕ from DER k, $i \in N, \phi \in \Phi(i)$ and $k \in K$. Similarly, $Q_{i\phi k}$ denotes the reactive power flow into node i in phase ϕ from DER k, $i \in N, \phi \in \Phi(i)$ and $k \in K$. For each phase ϕ, the sum of the power originated from DER k and sent to forward star of node i is equal to the power delivered to node i from DER k minus the power consumed at node i. Figure 4.2 displays a small network example to demonstrate these constraints. Since each phase is considered independent, the real and reactive power balance is enforced only for the nodes connected to that phase. For example, nodes j and l are the forward star of node i in phase a. To balance the real and reactive power flow, the remaining power at node i in phase a after power is consumed should be equal to the sum of the power supplied to the forward star nodes, i.e., nodes j and l. Similarly, for phases b and c, the power should be balanced for all the forward star nodes of node i connected in phases b and c, respectively. The power balance constraints can be represented as,

$$\sum_{j \in FS(i)} P_{j\phi k} = P_{i\phi k} - p_{i\phi} x_{i\phi k} \qquad i \in N, \phi \in \Phi(j), k \in K \quad (4.7)$$

$$\sum_{j \in FS(i)} Q_{j\phi k} = Q_{i\phi k} - q_{i\phi} x_{i\phi k} \qquad i \in N, \phi \in \Phi(j), k \in K \quad (4.8)$$

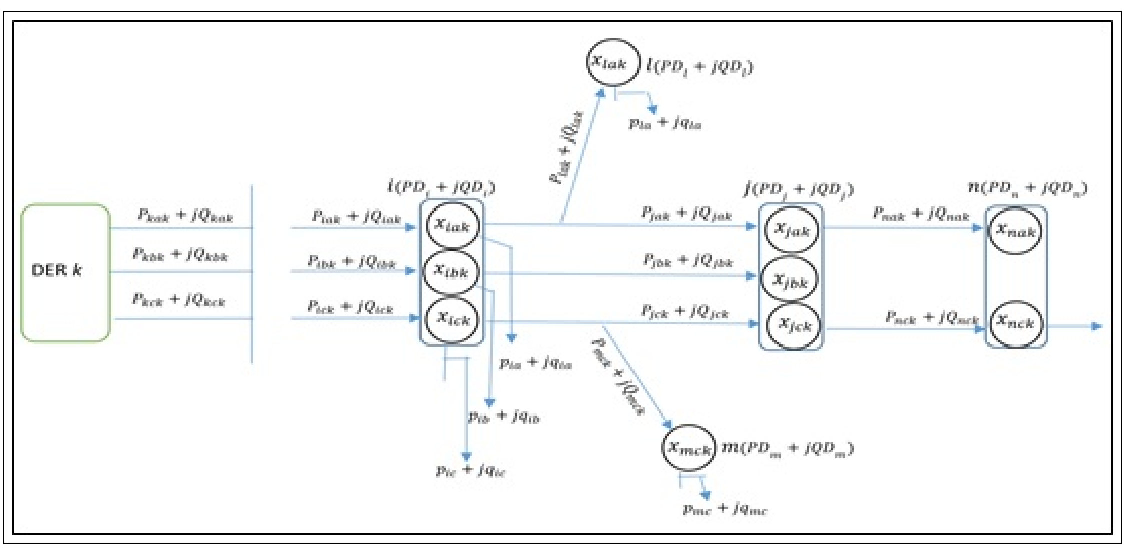

Figure 4.2: Phasewise real and reactive power balance for nodes

At any node i which is connected in the network, the power flow in phase ϕ should not be greater than the total capacity of the DER k connected to the node. If the node i is not connected in the network in phase ϕ from DER k, i.e., $x_{i\phi k} = 0$, then the power flow should be equal to zero. To ensure that only the nodes connected in the network are supplied, the following two constraints are used.

$$0 \leq P_{i\phi k} \leq P_k x_{i\phi k} \qquad i \in N, \phi \in \Phi(i), k \in K \quad (4.9)$$

$$0 \leq Q_{i\phi k} \leq Q_k x_{i\phi k} \qquad i \in N, \phi \in \Phi(i), k \in K \quad (4.10)$$

Where, P_k and Q_k are total real and reactive capacities available at DER k. For a DER node k, real and reactive power flows over all phases are limited by their capacities as follows,

$$\sum_{\phi \in \Phi(k)} P_{k\phi k} \leq P_k \qquad k \in K \quad (4.11)$$

$$\sum_{\phi \in \Phi(k)} Q_{k\phi k} \leq Q_k \qquad k \in K \quad (4.12)$$

In addition to the above power flow constraints, suppose that it is desirable that the power received at node i is evenly balanced over phases that the node is connected. To achieve this balanced power flows, we can enforce phase-dependent upper bounds on power flows that satisfy the demand at each node. Accordingly, let $\bar{p_{i\phi}}$ and $\bar{q_{i\phi}}$ denote these upper bounds. $\bar{p_{i\phi}}$ and $\bar{q_{i\phi}}$ are dependent on the number of phases the node i is connected. If node i is connected in three phases, i.e., $h_i = 3$, it is assumed that the maximum amount of real power supplied to node i becomes $\left(\frac{1}{3} + l\right) PD_i$, where $l \in (0, 1)$ an imbalance fraction by which the real power can vary. Likewise, for a node connected to two phases, i.e., $h_i = 2$, the maximum real power should be $\left(\frac{1}{2} + l\right) PD_i$. Note that, for a node i connected to a single phase, the real power should be equal to the entire demand at the node (PD_i). The same imbalance fraction can be applied to the reactive power. The constraints for $\bar{p_{i\phi}}$ and $\bar{q_{i\phi}}$ can be summarized as follows.

$$0 \leq p_{i\phi} \leq \bar{p_{i\phi}} \qquad i \in N, \phi \in \Phi(i) \quad (4.13)$$

$$0 \leq q_{i\phi} \leq \bar{q_{i\phi}} \qquad i \in N, \phi \in \Phi(i) \quad (4.14)$$

$$\text{where, } \bar{p_{i\phi}} = \left(\frac{1}{h_i} + l\right) PD_i \qquad i \in N, \phi \in \Phi(i) \quad (4.15)$$

$$\bar{q_{i\phi}} = \left(\frac{1}{h_i} + l\right) QD_i \qquad i \in N, \phi \in \Phi(i) \quad (4.16)$$

The variables $p_{i\phi}$ and $q_{i\phi}$ have a lower bound of zero. The sum of real and reactive power consumed by node i in all the phases i.e. $\sum_{\phi\in\Phi(i)} p_{i\phi}$ and $\sum_{\phi\in\Phi(i)} q_{i\phi}$, should be equal to the total real demand (PD_i) and reactive demand (QD_i) of node i, repectively. For example, if node i is connected to all the three phases abc, then the total real power demand (PD_i) must be equal to the sum of power consumption of node i in the three phases, i.e., $(p_{ia} + p_{ib} + p_{ic})$. These constraints are expressed as,

$$\sum_{\phi\in\Phi(i)} p_{i\phi} = PD_i \qquad i \in N/K \quad (4.17)$$

$$\sum_{\phi\in\Phi(i)} q_{i\phi} = QD_i \qquad i \in N/K \quad (4.18)$$

From equation 4.7 and 4.8, we can see that $(p_{i\phi}x_{i\phi k})$ and $(q_{i\phi}x_{i\phi k})$ are the products of a continuous and binary variables, which makes them nonlinear constraints. To linearize the nonlinear terms, we introduce two continuous variables $Z_{i\phi k}$ and $W_{i\phi k}$ for real power and reactive power flows, which replace nonlinear terms as follows.

$$\sum_{j \in FS(i)} P_{j\phi k} = P_{i\phi k} - Z_{i\phi k} \qquad i \in N, \phi \in \Phi(j), k \in K \quad (4.19)$$

$$\sum_{j \in FS(i)} Q_{j\phi k} = Q_{i\phi k} - W_{i\phi k} \qquad i \in N, \phi \in \Phi(j), k \in K \quad (4.20)$$

In order to ensure the substitutions are valid, we add the following linearization constraints [31].

$$0 \leq Z_{i\phi k} \leq p_{i\phi} \qquad i \in N, \phi \in \Phi(i), k \in K \quad (4.21)$$

$$Z_{i\phi k} \geq p_{i\phi} - \bar{p_{i\phi}}(1 - x_{i\phi k}) \qquad i \in N, \phi \in \Phi(i), k \in K \quad (4.22)$$

$$0 \leq Z_{i\phi k} \leq p_{i\phi} x_{i\phi k} \qquad i \in N, \phi \in \Phi(i), k \in K \quad (4.23)$$

$$0 \leq W_{i\phi k} \leq q_{i\phi} \qquad i \in N, \phi \in \Phi(i), k \in K \quad (4.24)$$

$$W_{i\phi k} \geq q_{i\phi} - \bar{q_{i\phi}}(1 - x_{i\phi k}) \qquad i \in N, \phi \in \Phi(i), k \in K \quad (4.25)$$

$$0 \leq W_{i\phi k} \leq q_{i\phi} x_{i\phi k} \qquad i \in N, \phi \in \Phi(i), k \in K \quad (4.26)$$

4.2.5 Phase Voltage Constraints

We consider that the voltage in the three phases a,b and c to be independent and any node connected in the network should be within the voltage tolerance limit in all the phases it is connected. $V_{i\phi k}$ represents the voltage at node i in phase ϕ connected to DER k. The linear approximation of voltage loss in an edge $(i, j, \phi, k) \in E$ can be expressed as,

$$V_{j\phi k} \leq V_{i\phi k} - \frac{r_{ij\phi k} P_{i\phi k} + s_{ij\phi k} Q_{i\phi k}}{RV_k} \qquad (i, j, \phi, k) \in E \quad (4.27)$$

In the constraint above, $r_{ij\phi k}$ and $s_{ij\phi k}$ denote the resistance and reactance of the edge $E(i, j, \phi, k)$ and RV_k denotes the reference voltage for the DER k. For DER nodes, we have

$$V_{k\phi k} = \nu \qquad k \in K, \phi \in \Phi(k) \quad (4.28)$$

The voltage for any node i connected in phase ϕ should be limited by the reference voltage of the DER k. On the other hand, if the node i is not connected, i.e., $x_{i\phi k} = 0$, the voltage must be zero.

$$0 \leq V_{i\phi k} \leq RV_k x_{i\phi k} \qquad i \in N, \phi \in \Phi(i), k \in K \quad (4.29)$$

To ensure that the voltage at any node i in all the phases it is connected in the network should be within the tolerance limit of the network, the following constraint is used,

$$(NV(1-t))x_{i\phi k} \leq V_{i\phi k} \leq (NV(1-t))x_{i\phi k} \qquad i \in N/K, \phi \in \Phi(i), k \in K \quad (4.30)$$

Where, NV denotes the nominal voltage of the network and and t represents the voltage tolerance limit of the network.

4.3 Notations

4.3.1 Variables

$$y_i = \begin{cases} 1 & \text{if node } i \text{ is connected,} \\ 0 & \text{otherwise} \end{cases}$$

$$i \in N$$

$$x_{i\phi k} = \begin{cases} 1 & \text{if node } i \text{ is connected in phase } \phi \text{ to DER } k, \\ 0 & \text{otherwise} \end{cases}$$

$$i \in N, \phi \in \Phi(i), k \in K$$

$P_{i\phi k}$ = real power flow into node i in phase ϕ from DER k,

$$i \in N, \phi \in \Phi(i), k \in K$$

$Z_{i\phi k}$ = continuous variable for real power consumption

$$i \in N, \phi \in \Phi(i), k \in K$$

$p_{i\phi}$ = real power consumption at node i in phase ϕ

$$i \in N, \phi \in \Phi(i)$$

$Q_{i\phi k}$ = reactive power flow into node i in phase ϕ from DER k,

$$i \in N, \phi \in \Phi(i), k \in K$$

$W_{i\phi k}$ = continuous variable for reactive power consumption

$$i \in N, \phi \in \Phi(i), k \in K$$

$q_{i\phi}$ = reactive power consumption at node $i$in phase ϕ

$$i \in N, \phi \in \Phi(i)$$

$V_{i\phi k}$ = voltage at node $i$in phase ϕ from DER k

$$i \in N, \phi \in \Phi(i), k \in K$$

4.3.2 Parameters

w_i = weight assigned to node i $\quad i \in N$

h_i = cardinality of $\Phi(i)$ ($h_i = |\Phi(i)|$) $\quad i \in N$

P_k = real capacity at DER k $\quad k \in K$

Q_k = reactive capacity at DER k $\quad k \in K$

PD_i = total real demand at node i $\quad i \in N$

QD_i = total reactive demand at node i $\quad i \in N$

$l = (0, 1)$Imbalance fraction by which power can vary

$r_{ij\phi k}$ = resistance in line *(i,j)*in phase ϕ $\quad (i, j) \in N, \phi \in \Phi(i), k \in K$

$s_{ij\phi k}$ = reactance in line *(i,j)* in phase ϕ $\quad (i, j) \in N, \phi \in \Phi(i), k \in K$

RV_k = reference voltage for DER k $\quad k \in K$

ν = initial voltage at the DER

NV = nominal voltage of the network

t = voltage tolerance limit of the network

4.4 Formulation

In summary, the three phase mixed integer linear formulation is as follows.

$$\text{Maximize} \quad \sum_{i \neq k} w_i y_i$$

subject to,

$$\sum_{k \in K} x_{i\phi k} \leq 1 \qquad i \in N/K, \phi \in \Phi(i)$$

$$x_{k\phi k} = 1 \qquad k \in K, \phi \in \Phi(k)$$

$$x_{j\phi k} \leq x_{i\phi k} \qquad (i, j, \phi, k) \in E$$

$$\sum_{k \in K} \sum_{\phi \in \Phi(i)} x_{i\phi k} = h_i y_i \qquad i \in N/K$$

$$y_i = 0 \qquad i \in F$$

$$\sum_{j \in FS(i)} P_{j\phi k} = P_{i\phi k} - Z_{i\phi k} \qquad i \in N, \phi \in \Phi(j), k \in K$$

$$\sum_{\phi \in \Phi(k)} P_{k\phi k} \leq P_k \qquad k \in K$$

$$0 \leq P_{i\phi k} \leq P_k x_{i\phi k} \qquad i \in N, \phi \in \Phi(i), k \in K$$

$$0 \leq p_{i\phi} \leq \bar{p_{i\phi}} \qquad i \in N, \phi \in \Phi(i)$$

$$\bar{p_{i\phi}} = \left(\frac{1}{h_i} + l \right) PD_i \qquad i \in N, \phi \in \Phi(i)$$

$$\sum_{\phi \in \Phi(i)} p_{i\phi} = PD_i \qquad i \in N$$

$$0 \leq Z_{i\phi k} \leq p_{i\phi} \qquad i \in N, \phi \in \Phi(i), k \in K$$

$$Z_{i\phi k} \geq p_{i\phi} - \bar{p_{i\phi}}(1 - x_{i\phi k}) \qquad i \in N, \phi \in \Phi(i), k \in K$$

$$0 \leq Z_{i\phi k} \leq p_{i\phi} x_{i\phi k} \qquad i \in N, \phi \in \Phi(i), k \in K$$

s.t.,

$$\sum_{j \in FS(i)} Q_{j\phi k} = Q_{i\phi k} - W_{i\phi k} \qquad i \in N, \phi \in \Phi(j), k \in K$$

$$\sum_{\phi \in \Phi(k)} Q_{k\phi k} \leq Q_k \qquad k \in K$$

$$0 \leq Q_{i\phi k} \leq Q_k x_{i\phi k} \qquad i \in N, \phi \in \Phi(i), k \in K$$

$$0 \leq q_{i\phi} \leq \bar{q_{i\phi}} \qquad i \in N, \phi \in \Phi(i)$$

$$\bar{q_{i\phi}} = \left(\frac{1}{h_i} + l\right) QD_i \qquad i \in N, \phi \in \Phi(i)$$

$$QD_i = \sum_{\phi \in \Phi(i)} q_{i\phi} \qquad i \in N$$

$$0 \leq W_{i\phi k} \leq q_{i\phi} \qquad i \in N, \phi \in \Phi(i), k \in K$$

$$W_{i\phi k} \geq q_{i\phi} - \bar{q_{i\phi}}(1 - x_{i\phi k}) \qquad i \in N, \phi \in \Phi(i), k \in K$$

$$0 \leq W_{i\phi k} \leq q_{i\phi} x_{i\phi k} \qquad i \in N, \phi \in \Phi(i), k \in K$$

$$V_{j\phi k} \leq V_{i\phi k} - \frac{r_{ij\phi k} P_{i\phi k} + s_{ij\phi k} Q_{i\phi k}}{RV_k} \qquad (i, j, \phi, k) \in E$$

$$V_{k\phi k} = \nu \qquad k \in K, \phi \in \Phi(k)$$

$$0 \leq V_{i\phi k} \leq RV_k x_{i\phi k} \qquad i \in N, \phi \in \Phi(i), k \in K$$

$$(NV(1-t)) x_{i\phi k} \leq V_{i\phi k} \leq (NV(1-t)) x_{i\phi k} \qquad i \in N/K, \phi \in \Phi(i), k \in K$$

CHAPTER 5: EXTENSIONS OF SINGLE PHASE FORMULATION

In this chapter, we propose two extensions to the single phase formulation. First, we replace the linear optimization of power balance equations with their nonlinear counterparts to reflect exact power flows. Next, for non-radial or meshed distribution networks we propose an algorithm to convert them into radial distribution networks, so they can be solved using the proposed formulation in Chapter 3.

5.1 Nonlinear Power Balance Formulation

The linearized power balance equations provide an approximation of the power flow in the distribution network. However, it does not take into consideration the power loss due to the resistance and reactance in the lines. In an actual distribution network, the power in the grid is governed by the nonlinear loss function. Comparing the nonlinear and linearized formulations for the single phase problem will help us get better insights on the actual working of the distribution network with DERs.

Consider, the same objective function and constraints as those for the linearized single phase formulation except for the constraints 3.7, 3.8 and 3.11. The nonlinear power balance equations of DistFlow Model in [29] are used here and modified to suit the problem. The nonlinear constraints to replace 3.7 and 3.8 can be expressed as,

$$\sum_{j \in FS(i)} P_{jk} = P_{ik} - p_i x_{ik} - r_i \left(\frac{P_{ik}^2 + Q_{ik}^2}{RV_k^2} \right) \qquad i \in N, k \in K \quad (5.1)$$

$$\sum_{j \in FS(i)} Q_{jk} = Q_{ik} - q_i x_{ik} - s_i \left(\frac{P_{ik}^2 + Q_{ik}^2}{RV_k^2} \right) \qquad i \in N, k \in K, \quad (5.2)$$

where P_{ik} = real power flow into node i *from DER* k $\quad i \in N, k \in K$

Q_{ik} = reactive power flow into node i *from DER* k $\quad i \in N, k \in K$

p_i = real power demand at node i $\quad i \in N$

q_i = reactive power demand at node i $\quad i \in N$

r_i = resistance at node i $\quad i \in N$

s_i = reactance at node i $\quad i \in N$

RV_k = reference voltage for DER k $\quad k \in K$

The additional terms $r_i\left(\frac{P_{ik}^2+Q_{ik}^2}{RV_k^2}\right)$ and $s_i\left(\frac{P_{ik}^2+Q_{ik}^2}{RV_k^2}\right)$ represent the real and reactive power losses in the line flowing into node i, respectively. As illustrated in Figure 5.1 real and reactive power flows into node i are actually equal to $\left(P_{ik} - r_i\left(\frac{P_{ik}^2+Q_{ik}^2}{RV_k^2}\right)\right) + j\left(Q_{ik} - s_i\left(\frac{P_{ik}^2+Q_{ik}^2}{RV_k^2}\right)\right)$. We remark that the loss can be more precisely expressed by replacing RV_k with V_{ik}. However, the problem becomes highly nonlinear and a solution may not be found due to its complexity. As far as the voltage is concerned, the

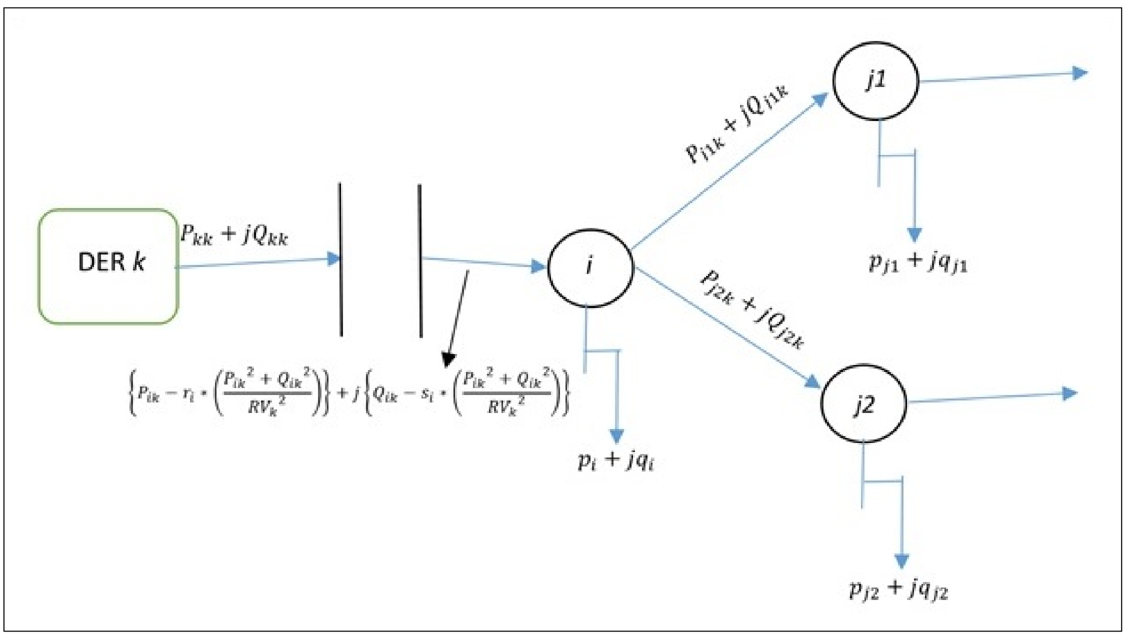

Figure 5.1: Nonlinear real and reactive power balance among nodes

linearized voltage constraint 3.11 is replaced by its nonlinear form as in the DistFlow

Model in [29]. For an edge $(i, j, k) \in E$, we have

$$V_{jk} \leq V_{ik} - 2(r_{ijk}P_{jk} + s_{ijk}Q_{jk}) - (r_{ijk}^2 + s_{ijk}^2)\left(\frac{P_{ik}^2 + Q_{ik}^2}{RV_k^2}\right) \qquad (i, j, k) \in E, \quad (5.3)$$

where V_{ik} = voltage at node i *connected to DER* k $\qquad i \in N, k \in K$

r_{ijk} = resistance in line *(i,j)* $\qquad (i, j) \in N, k \in K$

s_{ijk} = reactance in line *(i,j)* $\qquad (i, j) \in N, k \in K$

5.1.1 Nonlinear Formulation

The overall mixed integer nonlinear formulation is as follows.

$$\text{Maximize} \quad \sum_{i \neq k} w_i y_i$$

subject to,

$$\sum_{k \in K} x_{ik} \leq 1 \qquad i \in N/K$$

$$x_{kk} = 1 \qquad k \in K$$

$$x_{jk} \leq x_{ik} \qquad (i, j, k) \in E$$

$$y_i = \sum_{k \in K} x_{ik} \qquad i \in N/K$$

$$y_i = 0 \qquad i \in F$$

$$\sum_{j \in FS(i)} P_{jk} = P_{ik} - p_i x_{ik} - r_i \left(\frac{P_{ik}^2 + Q_{ik}^2}{RV_k^2} \right) \qquad i \in N, k \in K$$

$$0 \leq P_{ik} \leq P_k x_{ik} \qquad i \in N, k \in K$$

$$\sum_{j \in FS(i)} Q_{jk} = Q_{ik} - q_i x_{ik} - s_i \left(\frac{P_{ik}^2 + Q_{ik}^2}{RV_k^2} \right) \qquad i \in N, k \in K$$

$$0 \leq Q_{ik} \leq Q_k x_{ik} \qquad i \in N, k \in K$$

$$V_{jk} \leq V_{ik} - 2(r_{ijk} P_{jk} + s_{ijk} Q_{jk}) - (r_{ijk}^2 + s_{ijk}^2) \left(\frac{P_{ik}^2 + Q_{ik}^2}{RV_k^2} \right) \qquad (i, j, k) \in E$$

$$V_{kk} = \nu \qquad k \in K$$

$$0 \leq V_{ik} \leq RV_k x_{ik} \qquad i \in N, k \in K$$

$$(NV(1-t)) x_{ik} \leq V_{ik} \leq (NV(1-t)) x_{ik} \qquad i \in N/K, k \in K$$

5.2 Conversion of Meshed to Radial Network

Recall that the distribution network considered so far is radial, i.e., each node has only parent node. However, meshed or non-radial networks are not uncommon in practice. To be able to use the above proposed formulations with non-radial networks, we propose a method to convert non-radial to radial networks by solving shortest path problem where distances are represented as line lengths. The shortest path problem aims at finding the shortest distance from a source to sink node in a graph. We propose using the Dijkstra's algorithm [32], which efficiently finds the minimum distances between the sources (DER) to all the other nodes connected in the network.

Assume that the length of the line connecting two nodes is directly proportional to the amount of power loss in the line. In a distribution network, line lengths are known parmaeters. Since we consider multiple DER sources in the network, the shortest path problem needs to be solved for each DER connected in the network. We demonstrate the proposed problem using a small example shown below in Figure 5.2. Consider two DERs in the network acting as the source and the lines connecting the nodes in the network with known distances. Note that, there exist multiple paths from each DER to a node. Among those possible paths we select the path that has the shortest distance from each DER. For example, node 3 can be supplied by multiple paths from DER 1. The different paths and distances from DER 1 to node 3 are listed in Table 5.1. The shortest path from DER 1 to node 3 will be $D1 - 1 - 3$ with a distance of 17.

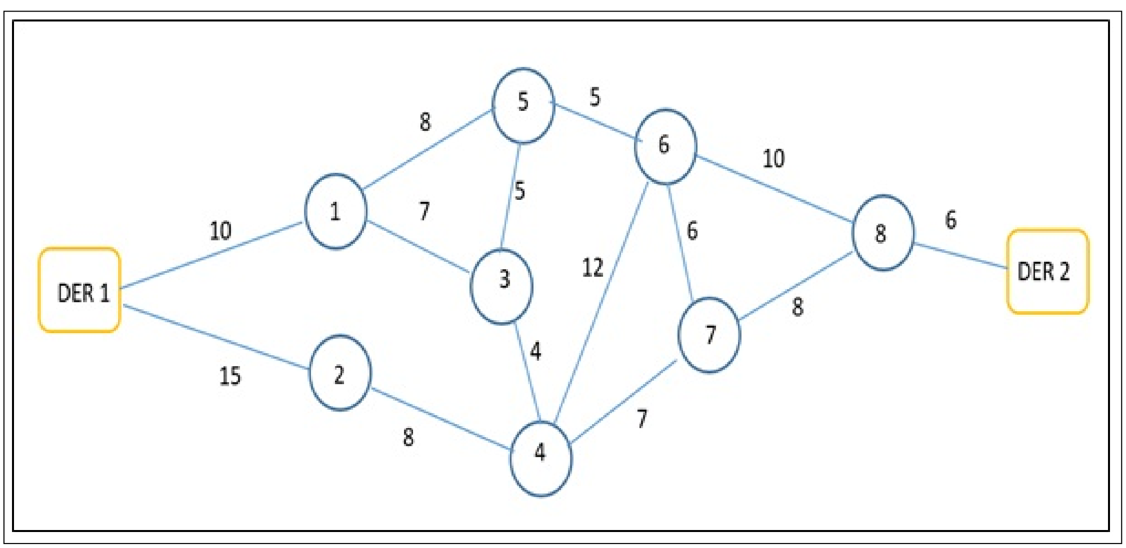

Figure 5.2: Meshed network example

Table 5.1: Paths from DER 1 to node 3

Paths	Distance
D1-1-3	17
D1-1-5-3	23
D1-1-5-6-4-3	39
D1-1-5-6-7-4-3	40
D1-1-5-6-8-7-4-3	52
D1-2-4-3	27
D1-2-4-7-6-5-1-3	56
D1-2-4-7-6-5-3	46
D1-2-4-7-8-6-5-1-3	68
D1-2-4-7-8-6-5-3	58

When we consider one DER 1 as the source, other DERs would be considered as load points in the network. The shortest path to all the nodes considering DER 1 and DER 2 as the source are shown in Figure 5.3 and 5.4 respectively.

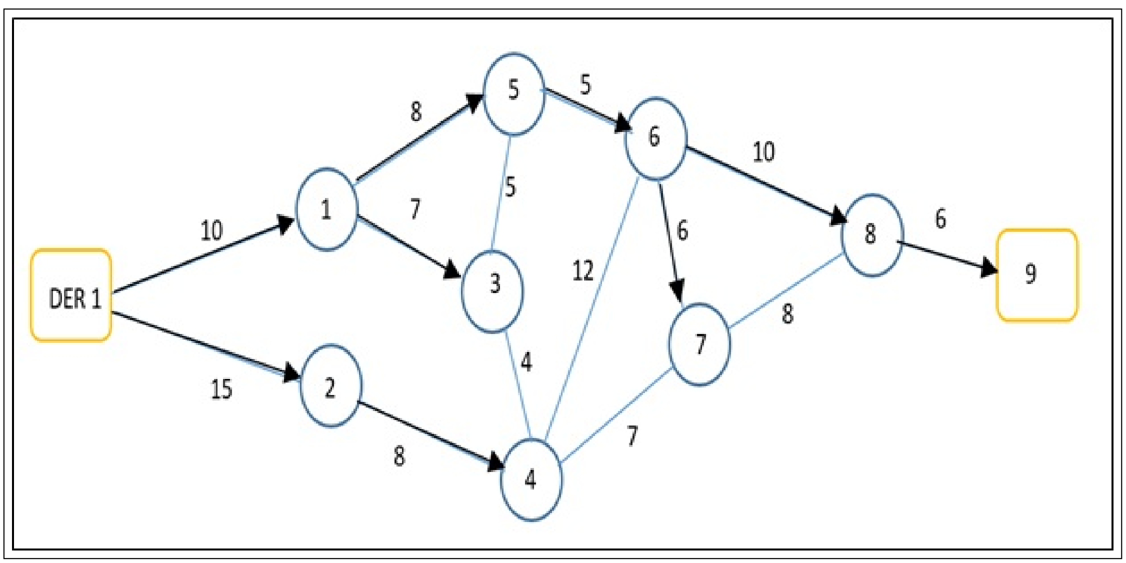

Figure 5.3: Construction of radial network for DER 1

As seen from Figure 5.3 and 5.4 for DER 1 and DER 2 as the sources, the shortest paths to all the nodes in the network constitute respective radial networks. In general, for a real feeder system where multiple DERs are located, the shortest paths to all the nodes from each DER in the network can serve as radial distribution networks. Once the paths are identified for each DER, they can be input into the single phase formulation as the set of edges. For a three phase distribution network, the paths for all the nodes in the network needs to be identified for each DER in all the phases it is connected. By using the shortest path algorithm, we can transform a meshed network into a radial network for it to be used with the formulations proposed in Chapter 3 and 4.

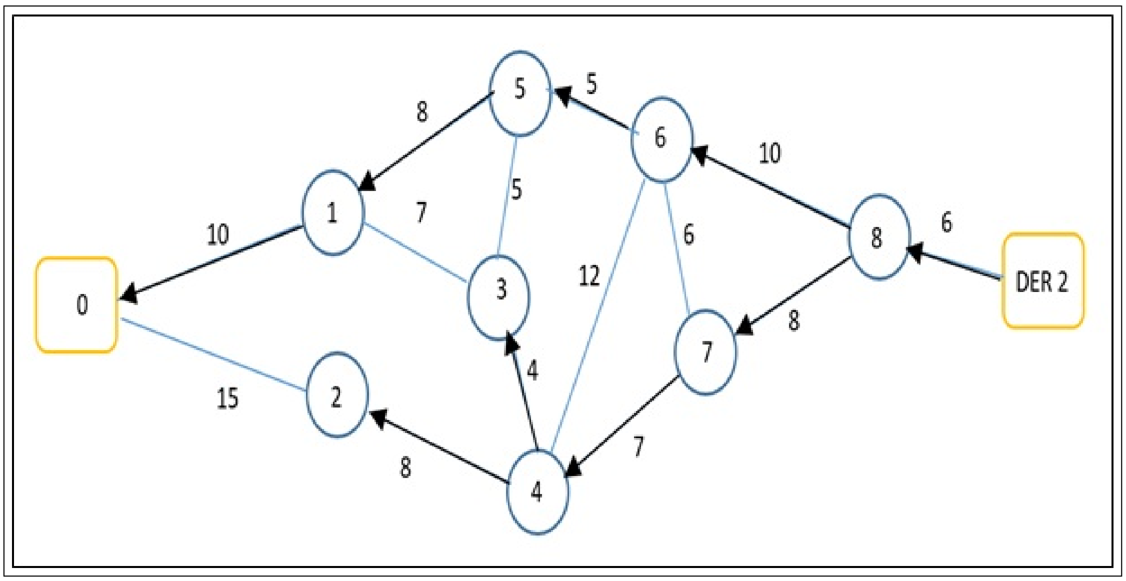

Figure 5.4: Construction of radial network for DER 2

CHAPTER 6: NUMERICAL RESULTS

In this chapter, the results for all the three formulations are presented. The chapter is divided in two main sections one for the single phase formulation and second for three phase formulation. An operational distribution network from utility in North Carolina is taken to demonstrate the results for both formulations. The distribution network in consideration is shown in Figure 6.1. Various fault scenarios and DER placements are considered for both formulations. The network in consideration here consisted of 248 node points with 97 of them as load points. Four DERs are placed at four different node points in the distribution network. The DER locations considered are shown in Figure 6.1.

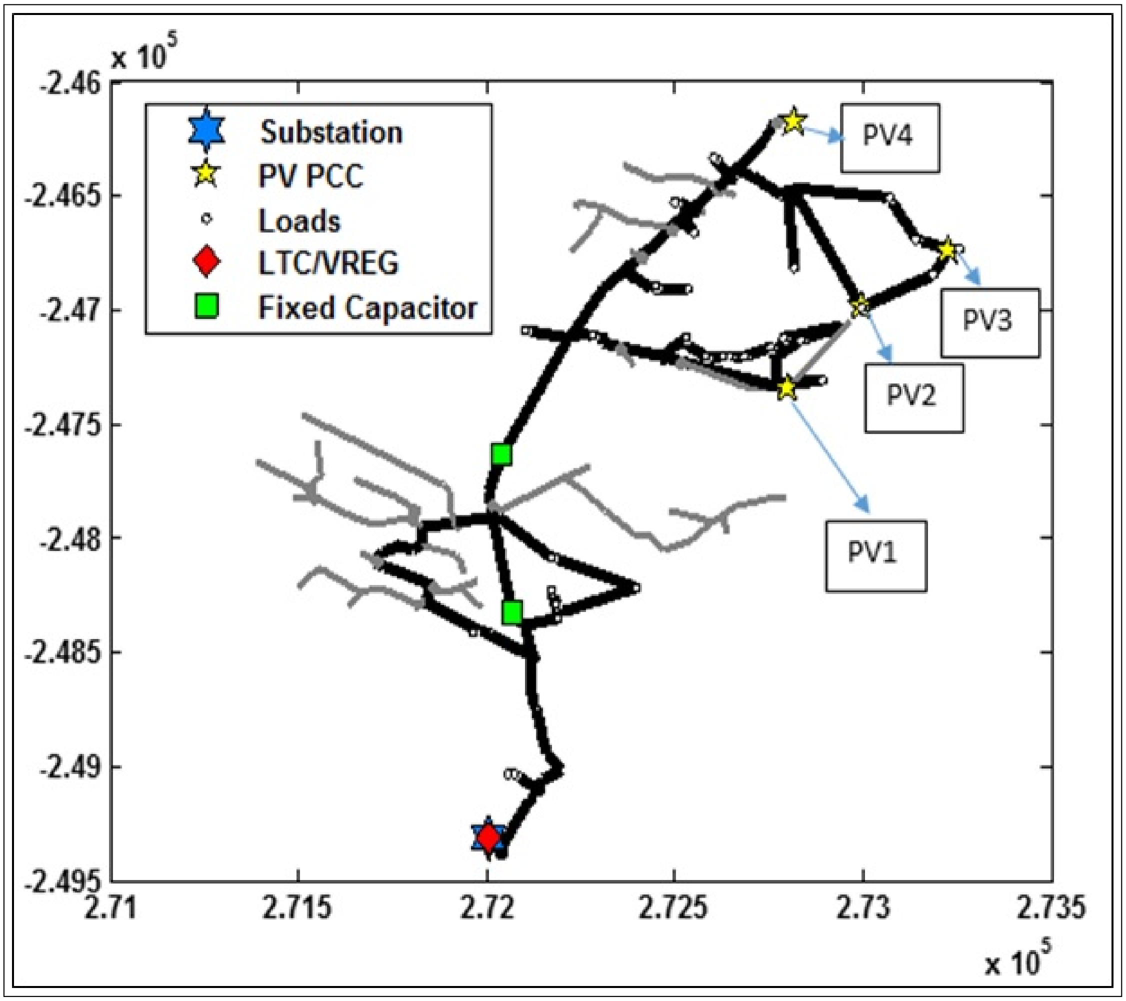

Figure 6.1: Example distribution network

The power demand at each of the 97 load points was known from the utility data. The real and reactive demands at the nodes is taken as 0.9 and 0.1 of the overall demand at the nodes. The real and reactive capacity of all the DERs combined is taken as 40% of the total real and reactive demand of all the nodes in the network respectively. The voltage tolerance limit of the distribution network is taken as 5%. Though, under emergency conditions a higher tolerance limit can be considered, for the purpose of this problem we consider a 5% tolerance limit. The star in Figure 6.1 above represents the substation node. It is considered that under normal operational conditions, the substation would be supplying the distribution network and the DER nodes will be supplying its own load demand. In times of emergency or faults in the line, the DER nodes will be first satisfying their own demand and then supplying the additional power available to supply the nearby nodes based on their weight priority. Hence, the DER nodes are excluded from the objective function value of the formulations.

Since the objective function of both the models in consideration are same, similar weight priorities are assigned for both, the single phase and three phase formulation. The weight priorities on the nodes are chosen randomly since the exact location of the important load points such as Hospitals, Schools, Fire Stations, Police Stations, etc. were unknown. 26 out of the 97 load points were considered as high priority nodes with a weight of 1000. The remaining 71 load points are considered as the second priority level nodes and assigned a weight of 100. The remaining nodes in the distribution network have no load demand and only pass the power to the next node connected in the series. These type of nodes are assigned a weight of 0. Since the power available at the DERs is only 40.59% of the total demand, all the nodes in the distribution network would not be supplied and the optimization routine would aim towards supplying the high priority node points with a weight of 1000. The following sub-sections explain in detail the results from both the formulations.

6.1 Single Phase Distribution Network Results

Two scenarios are considered here, one with the multiple faults in the distribution network. Second with the major fault scenario, where the substation is disconnected from the distribution network during a storm.

6.1.1 Single Phase Multiple Faults Scenario

In scenario of an extreme natural calamity, multiple faults are usually observed in a distribution network. This scenario considers multiple random faults of the main line of the feeder system in consideration. In particular, three permanent faults are considered on the main line in the distribution network disconnecting the load points from the feeder. As discussed earlier four DER locations are considered. The fault and the DER locations are shown in in Figure 6.2.

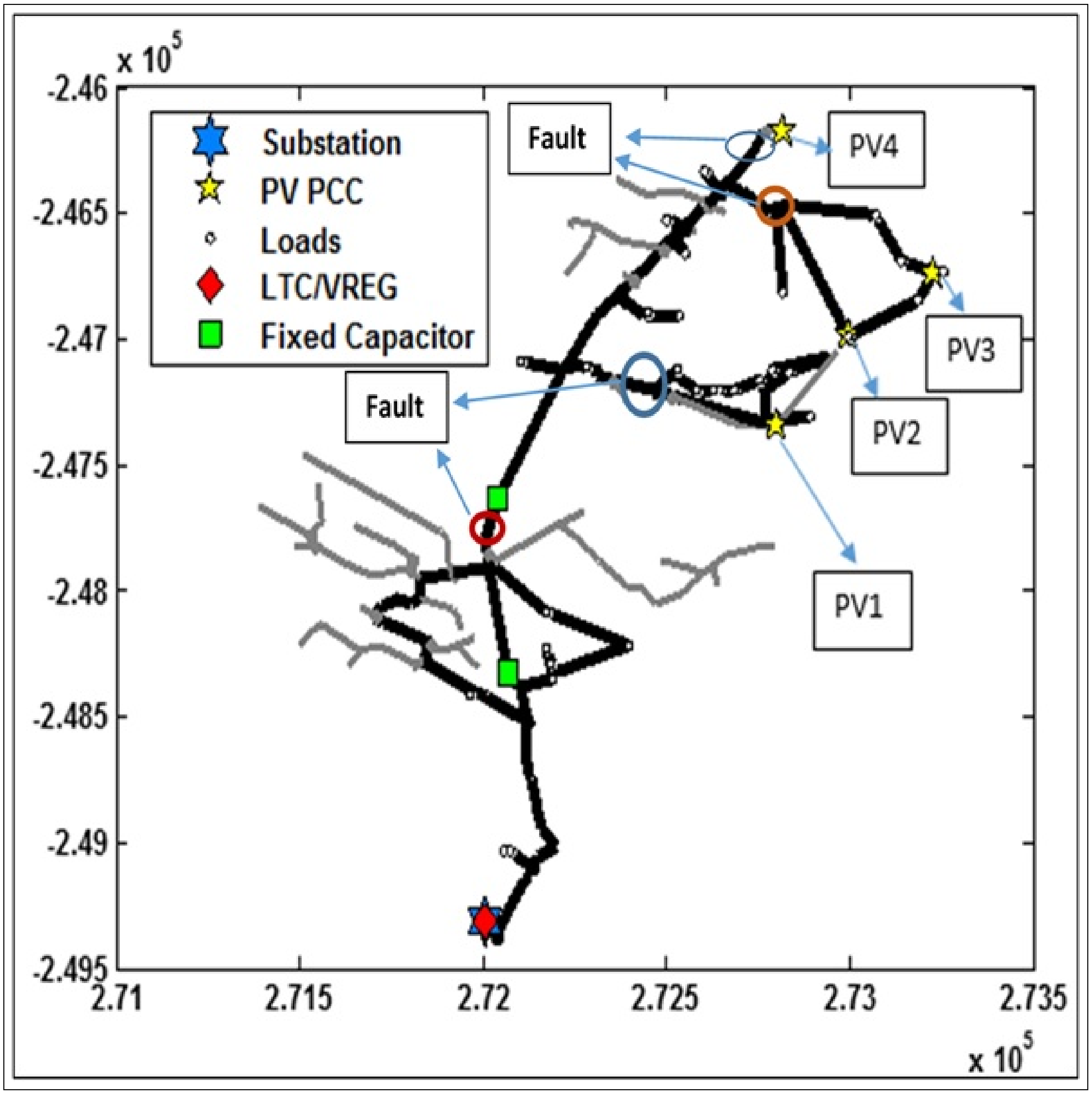

Figure 6.2: Multiple fault scenario location in sample distribution network

The real and reactive power considered at the DER is shown in Table 6.1. The initial voltage at the DER nodes (V_{kk}), reference voltage (RV_k) and nominal voltage (NV) is taken as 7.2 KV. A voltage tolerance limit of 5% ($t = 0.05$) is considered for the distribution network. Any node connected to the network should be within the upper and lower voltage tolerance limits. The resistance and reactance values of each edge in the network is calculated based on the line type and the line length.

The optimization model was coded in AMPL [33] and solved by the IBM Ilog

Table 6.1: Real and reactive power capacity at DERs (single phase multiple fault scenario)

DER	Real Power Capacity (KVA)	Reactive Power Capacity (Kvar)
PV1	1710	190
PV2	2403	267
PV3	2493	277
PV4	198	22
Total	6804	756

Table 6.2: Real and reactive power supplied by DERs (single phase multiple faults scenario)

DER	Real Power Capacity (KVA)	Reactive Power Capacity (Kvar)
PV1	1125.18	125.02
PV2	2187.18	243.02
PV3	2475.09	275.01
PV4	45	5
Total	5832.45	648.05

CPLEX solver [34] using the NEOS Kestrel Server [35], [36], [37], [38]. The simulation environment used is of Intel Xeon $X5660$ 2.8 GHz with 64 GB memory. The preprocessing of the CPLEX solver reduced the number of variables from 4216 to 508 (202 binary and 306 continuous). The number of constraints reduced from $10,395$ to 1005 constraints. The problem was solved to optimality with an objective value of 14600 in 145 MIP simplex iterations. The total real power and reactive power supplied from the four DERs is 5832.45 KVA and 648.05 Kvar out of the total available 6804 KVA and 756 Kvar, respectively. 12 of the 18 high priority loads situated in the faulty zone were supplied by the DERs. The total real and reactive power supplied from the DERs are shown in Table 6.2 and the 12 high priority loads served by the four DERs in the distribution network and their real and reactive power consumption are shown in Table 6.3.

Table 6.3: High priority loads served from DERs (single phase multiple faults scenario)

Node No.	**Real Power Demand (KVA)**	**Reactive Power Served (Kvar)**
142	202.5	22.5
148	135	15
153	450.09	50.01
155	450.09	50.01
168	135	15
169	450.09	50.01
170	1350	150
171	450.09	50.01
179	202.5	22.5
232	450.09	50.01
245	675	75

For the second priority level nodes, 26 out of the 28 nodes were served in the network. The voltages for the nodes connected are plotted in ascending order to check for any violations. The voltage for most of the nodes shown is towards the lower limit of the tolerance because of the inequality we consider in our voltage power balance equation.

The resulting network after the optimization routine considering the four faults can be seen in Figure 6.3, where each DER and corresponding area being served by the DER are displayed by respective color. As it can be seen from Figure 6.3, each of the DER supplies its neighboring nodes to form its own micro-grid. Lines with black color are loads connected to the sub-station. Lines with gray color could not be served by DERs due to their limited capacities.

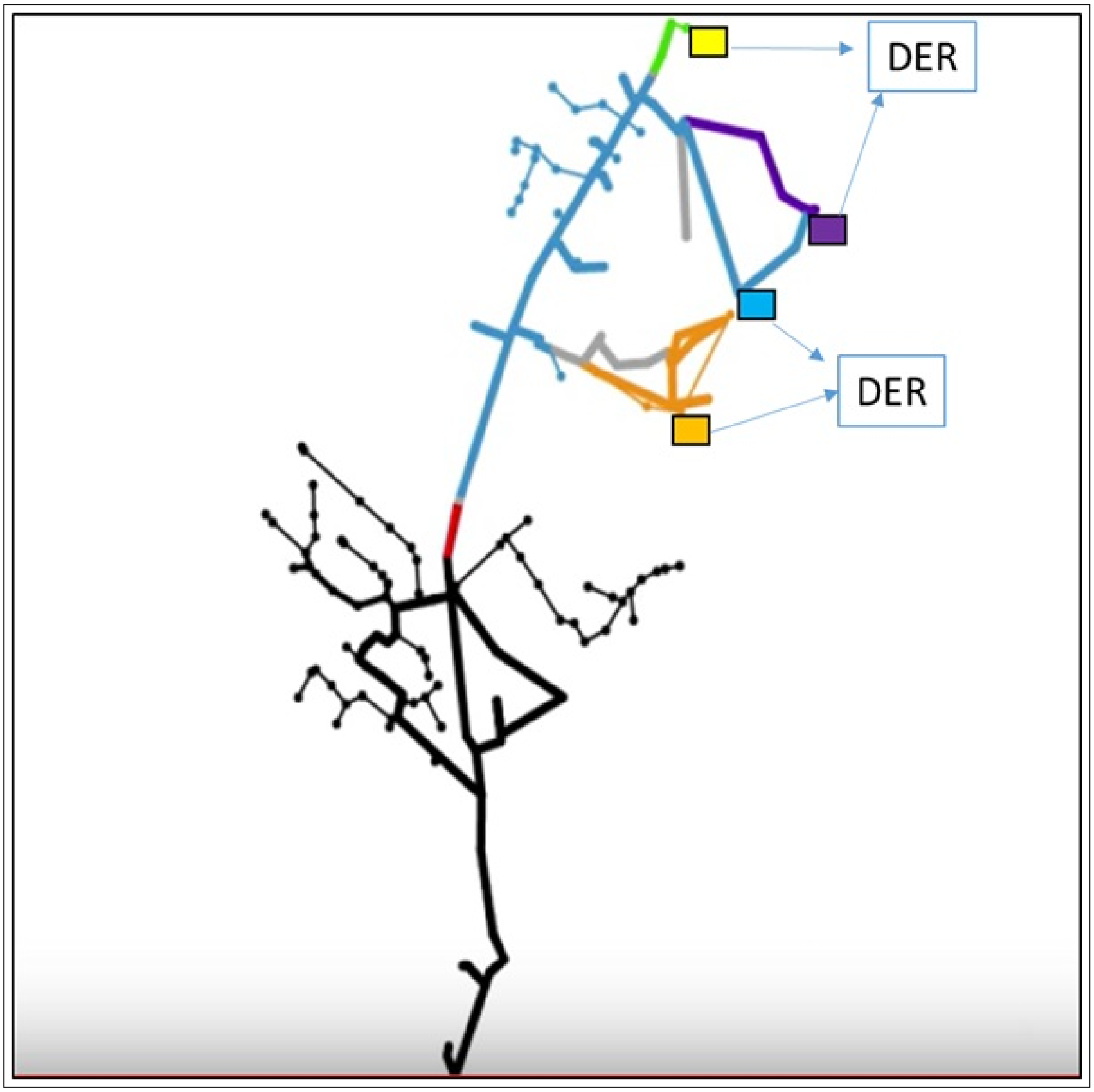

Figure 6.3: Result of single Phase Multiple Fault scenario

6.1.2 Single Phase Major Fault Scenario

For the major fault scenario, we consider a fault that occurs near the substation node and results in power outage of the entire distribution network. The fault locations are shown in the Figure 6.4 The location of the DERs are the same as in the first scenario.

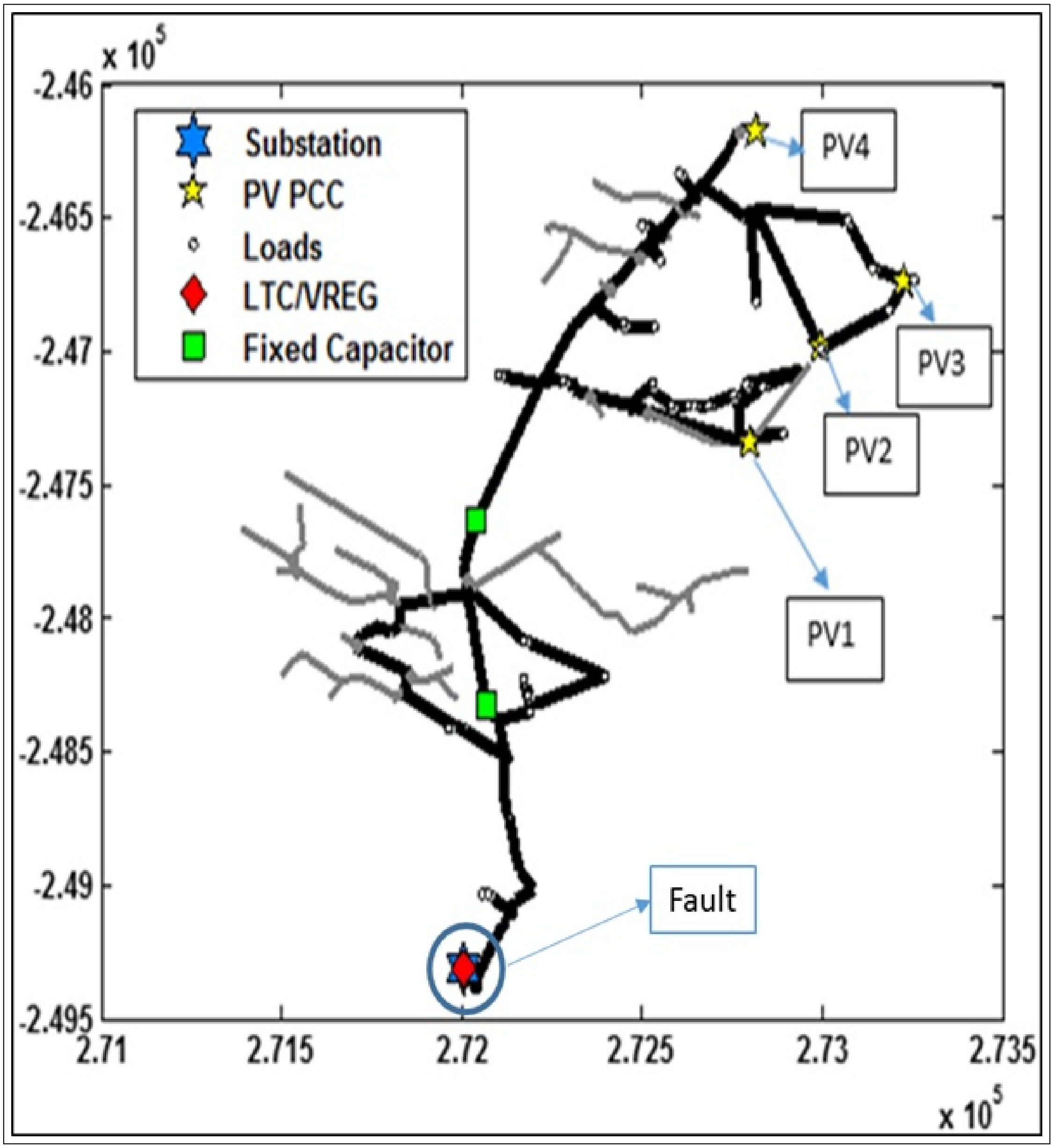

Figure 6.4: Major fault Scenario location in sample distribution network

As in the previous scenario, we use the same four DER capacities and same weight priorities for the nodes. The preprocessing of the CPLEX solver reduced the number of variables from 4216 to 2391 (806 binary and 1585 Continuous). The number of constraints reduced from 10,395 to 5321 constraints. The problem was solved to optimality with an objective value of 18900 after 1133 MIP iterations. The total real power and reactive power supplied from the four DERs is 6453.36 KVA and 717.04

Table 6.4: Real and reactive power supplied by DERs (single phase major fault scenario)

DER	Real Power Capacity (KVA)	Reactive Power Capacity (Kvar)
PV1	1516.68	168.52
PV2	2394.09	266.01
PV3	2475.09	275.01
PV4	67.5	7.5
Total	6453.36	717.04

Kvar out of the total available 6804 KVA and 756 Kvar respectively. 15 of the 26 high priority and 39 of the 71 second priority loads were supplied by the DERs. The real and reactive power supplied and the high priority nodes served are is shown in Table 6.4 and 6.5, respectively.

6.2 Nonlinear Multiple Faults Scenario Results

In this section, we present the results for the nonlinear single phase formulation proposed in Chapter 5. We consider the same multiple faults scenario as for the linearized single phase formulation. The same DER locations and capacities are considered and same weight priorities for the nodes are assigned. The optimization model was coded in AMPL [33] and solved by the BARON [39] using the NEOS Kestrel Server [35], [36], [37], [38].

The preprocessing of the solver reduced the number of variables from 4216 to 570 (223 binary and 347 continuous). The number of constraints reduced from $10,395$ to 1138 constraints out of which 356 were non-linear constraints. The problem was solved to optimality with an objective value of 13400 with 8 iterations. The total real power and reactive power supplied from the four DERs is 4457.982 KVA and 502.3866 Kvar out of the total available 6804 KVA and 756 Kvar, respectively. 11 of the 18 high priority loads and 24 of the 28 second priority loads were supplied by the DERs in the network.

Table 6.5: High priority loads served from DERs (single phase major fault scenario)

Node No.	**Real Power Demand (KVA)**	**Reactive Power Served (Kvar)**
96	90	10
142	202.5	22.5
143	270	30
148	135	15
153	450.09	50.01
155	450.09	50.01
161	135	15
168	135	15
169	450.09	50.01
171	450.09	50.01
175	450.09	50.01
179	135	15
180	202.5	22.5
232	450.09	50.01
245	675	75

Table 6.6: Power Supplied by DERs (nonlinear multiple faults scenario)

DER	**Real Power Capacity (KVA)**	**Reactive Power Capacity (Kvar)**
PV1	1132.55	127.917
PV2	1577.87	176.07
PV3	1702.56	193.393
PV4	45	5
Total	4457.98	502.38

In comparison to the linearized single phase results, the DERs do not supply one high priority load and two second priority loads were not supplied due to the power loss and the voltage tolerance of the network. Since this scenario is relatively small scale, it could be solved to optimality. But in scenarios where the problem size is larger, we observed the solution failed to converge. Fora relatively large scale problems, the linearized version serves as a good estimate and can be used for a quick solution.

6.3 Three Phase Distribution Network Results

We consider the same distribution network with the nodes connected in three, two or single phases. For the three-phase network formulation presented in Chapter 4, we consider four scenarios. First, we consider the two scenarios with multiple local faults and major fault scenario where two DERs connected in all three phases, i.e., abc and other two DERs connected only in single phases namely b and c. Next, we consider the two scenarios the multiple local faults and major fault scenarios where all the DERs connected in three phases, i.e., abc. Numerical results for each scenario are presented in the respective sub-sections below.

6.3.1 Mixed Phase Multiple Faults Scenario

In this scenario, we consider the same fault and DER locations as shown in Figure 6.2. But, the $PV1$ and $PV4$ are connected in phase b and c, respectively. $PV2$ and $PV3$ are connected in all three phases abc. The phases in which the DERs are connected and their real and reactive power capacities are summarized in Table 6.7.

The preprocessing of the CPLEX solver reduced the number of variables from $10,252$ to 1358 (289 binary and 1069 continuous). The number of constraints reduced from $24,613$ to 2432 constraints. The problem was solved to optimality with an objective value of 11300 in 999 MIP iterations. The total real power and reactive power supplied from the four DERs is 4684.773 KVA and 520.53 Kvar out of the total available 6804 KVA and 756 Kvar respectively. 9 of the 18 high priority loads and 23 out of the 28 second priority loads in the faulty zone were supplied by the DERs. The

Table 6.7: Power Capacity of DER (mixed phase multiple fault scenario)

DER	Phases	Real Power Capacity (KVA)	Reactive Power Capacity (Kvar)
PV1	*b*	1710	190
PV2	*abc*	2403	267
PV3	*abc*	2493	277
PV4	*c*	198	22
Total		6804	756

Table 6.8: Power supplied by DER (mixed phase multiple fault scenario)

DER	Phases	Real Power Capacity (KVA)	Reactive Power Capacity (Kvar)
PV1	*b*	22.5	2.5
PV2	*abc*	2187.18	243.02
PV3	*abc*	2475.09	275.01
PV4	*c*	0	0
Total		4684.77	520.53

total real and reactive power supplied from the DERs are shown in Table 6.8.

The amount of real and reactive power supplied by the DERs in each phase in shown in Table 6.9 and 6.10 respectively. $PV1$ and $PV4$ are only connected to phase b and c, respectively. Hence, no power is supplied by the two DERs in other phases. The DERs PV2 and PV3 are connected in all the three phases and hence supply majority of the real and reactive power available as shown in Table 6.9 and 6.10.

Table 6.9: Real power consumption (mixed phase multiple fault scenario)

DER	***Phase a***	***Phase b***	***Phase c***
PV1		22.5	
PV2	980.24	654.41	552.53
PV3	1023.04	915.016	537.037
PV4			0

Table 6.10: Reactive power consumption (mixed phase multiple fault scenario)

DER	*Phase a*	*Phase b*	*Phase c*
PV1		2.5	
PV2	109.515	87.5949	45.9101
PV3	113.671	113.671	47.6684
PV4			0

Table 6.11: Power supplied by DER (three phase multiple faults scenario)

DER	Phases	Real Power Capacity (KVA)	Reactive Power Capacity (Kvar)
PV1	*abc*	1395.17	155.02
PV2	*abc*	2187.18	243.02
PV3	*abc*	2475.09	275.01
PV4	*abc*	45	5
Total		4684.77	520.53

6.3.2 Three Phase Multiple Faults Scenario

In this scenario, all the four DERs are considered connected in three phases. The real and reactive capacity of the DERs in the distribution network are the same as the previous scenario (see Table 6.7).

The preprocessing of the CPLEX solver reduced the number of variables from $14,782$ to 1660 (363 binary and 1297 continuous). The number of constraints reduced from $35,896$ to 3106 constraints. The problem was solved to optimality with an objective value of 15700 in 719 MIP iterations. The total real power and reactive power supplied from the four DERs is 5832.448 KVA and 648.05 Kvar out of the total available 6804 KVA and 756 Kvar respectively. 13 of the 18 high priority loads and 27 out of the 28 second priority loads in the faulty zone were supplied by the DERs. The real and reactive power supplied and the high priority nodes served are is shown in Table 6.11 and 6.20, respectively.

Table 6.12: High priority loads served from DERs (three phase multiple faults scenario)

Node	***Phase a***		***Phase b***		***Phase c***	
	Real Power (KVA)	**Reactive Power (Kvar)**	**Real Power (KVA)**	**Reactive Power (Kvar)**	**Real Power (KVA)**	**Reactive Power (Kvar)**
142	83.7	9.3	83.7	3.9	35.1	9.3
148	55.8	6.2	55.8	2.6	23.4	6.2
153	186.037	8.6684	78.0156	20.6708	186.037	20.6708
155	186.037	8.6684	78.0156	20.6708	186.037	20.6708
168	55.8	6.2	55.8	6.2	23.4	2.6
169	186.037	20.6708	186.037	20.6708	78.0156	8.6684
170	450	50	450	50	450	50
171	150.03	16.67	150.03	16.67	150.03	16.67
175	46.8	5.2	111.6	12.4	111.6	12.4
179	55.8	6.2	23.4	6.2	55.8	2.6
180	83.7	9.3	35.1	9.3	83.7	3.9
232	186.037	20.6708	186.037	20.6708	78.0156	8.6684
245	225	25	225	25	225	25

Table 6.13: Real power consumption (three phase multiple faults sceanario)

DER	***Phase a***	***Phase b***	***Phase c***
PV1	502.57	357.63	534.94
PV2	971.59	718.15	497.43
PV3	825.03	825.03	825.03
PV4	7.8	18.6	18.6

Table 6.14: Reactive power consumption (three phase multiple faults sceanario)

DER	***Phase a***	***Phase b***	***Phase c***
PV1	31.83	61.94	61.24
PV2	105.79	84.11	53.11
PV3	91.67	91.67	91.67
PV4	0.87	2.07	2.07

Since all the DERs are connected in three phases, they have more flexibility to supply all the three phase nodes as well as the nodes connected to two and single phases. Thus, more load points in the distribution network can be supplied by the DERs as compared to the scenario considered above. The power demand in all the phases is split up evenly and balanced over phases the node is connected. The real and reactive power supplied by the DERs in each phase are presented in Table 6.13 and 6.14.

From Table 6.13 and 6.14, it can be seen that the real and reactive power are supplied in all the three phases for all the DERs. The real and reactive power is independently balanced for each phase based on the load point power demand.

6.3.3 Mixed Phase Major Fault Scenario

We consider the same major fault scenario as shown in Figure 6.4. The same DER phases and real and reactive capacity are shown in 6.7. The preprocessing of the CPLEX solver reduced the number of variables from $10,252$ to 4507 (1104 binary and 3403 continuous). The number of constraints reduced from $24,613$ to 9931

Table 6.15: Power supplied by DER (mixed phase major fault scenario)

DER	**Phases**	**Real Power Capacity (KVA)**	**Reactive Power Capacity (Kvar)**
PV1	*b*	1709.46	189.94
PV2	*abc*	2403	267
PV3	*abc*	2492.99	276.99
PV4	*c*	27.9	3.1
Total		6633.35	737.03

Table 6.16: Real power consumption (mixed phase major fault sceanario)

DER	***Phase a***	***Phase b***	***Phase c***
PV1		1709.46	
PV2	1083.29	0	1319.71
PV3	926.91	357.01	1209.07
PV4			27.9

constraints. The problem was solved to optimality with an objective value of 19100 in 46507 MIP iterations and 268 branch-and-bound nodes. The total real power and reactive power supplied from the four DERs is 6633.356 KVA and 737.03 Kvar out of the total available 6804 KVA and 756 Kvar respectively. 14 of the 26 high priority loads and 51 out of the 71 second priority loads were supplied by the DERs. The total real and reactive power supplied from the DERs are displayed in Table 6.15.

The real and reactive power supplied by the DERs in each phase are presented in Table 6.16 and 6.17, respectively. Since all of the load points are in the faulty section, there are more feasible configurations to connect DERs and hence, more real and reactive power can be supplied by the DERs in comparison to multiple faults scenario.

6.3.4 Three Phase Major Fault Scenario

The major fault scenario is considered here. The DER real and reactive capacity are taken from the Table 6.7 but all the DERs are connected in three phase. The

Table 6.17: Reactive power consumption (mixed phase major fault sceanario)

DER	***Phase a***	***Phase b***	***Phase c***
PV1		189.94	
PV2	150.967	0	116.033
PV3	122.339	33.6708	120.99
PV4			3.1

Table 6.18: Power supplied by DER (three phase major fault scenario)

DER	Phases	Real Power Capacity (KVA)	Reactive Power Capacity (Kvar)
PV1	*abc*	1710	189.83
PV2	*abc*	2403	267
PV3	*abc*	2475.09	275.01
PV4	*abc*	196.47	22
Total		6784.56	753.84

preprocessing of the CPLEX solver reduced the number of variables from 14,692 to 7241 (1707 binary and 5534 continuous). The number of constraints reduced from 35,897 to 16,423 constraints. The problem was solved to optimality with an objective value of 20900 in 962984 MIP iterations and 2923 branch-and-bound nodes. The total real power and reactive power supplied from the four DERs is 6784.56 KVA and 753.84 Kvar out of the total available 6804 KVA and 756 Kvar respectively. 15 of the 26 high priority loads and 59 out of the 71 second priority loads were supplied by the DERs. The real and reactive power supplied by the DERs in each phase are presented in Table 6.18 and 6.19.

Since, all the DERs are connected in three phases in this scenario, more real and reactive power is supplied by the DERs in comparison to the major fault with mixed phase scenario. The real and reactive power supplied by the DERs in each phase are presented in Table 6.20 and 6.21, respectively. The real and reactive loads in all the phases are balanced based on the weights priority of the load points connected in the

Table 6.19: High priority loads served from DERs (three phase major fault scenario)

Node	***Phase a***		***Phase b***		***Phase c***	
	Real Power (KVA)	**Reactive Power (Kvar)**	**Real Power (KVA)**	**Reactive Power (Kvar)**	**Real Power (KVA)**	**Reactive Power (Kvar)**
96	90	10				
142	50.07	8.99	68.73	4.20	83.7	9.3
143	46.8	12.4	111.6	12.4	111.6	5.2
148	39.6	6.2	39.6	6.2	55.8	2.6
153	132.02	20.67	132.02	20.67	186.03	8.66
155	132.02	20.67	132.02	20.67	186.03	8.66
161	55.8	2.6	52.12	6.2	27.07	6.2
168	55.8	6.2	55.8	2.6	23.4	6.2
170	558	62	558	26	234	62
171	186.03	20.67	78.01	8.66	186.03	20.67
175	111.6	12.4	111.6	5.2	46.8	12.4
179	55.8	2.6	23.4	6.2	55.8	6.2
180	83.7	6.15	35.1	7.04	83.7	9.3
232	186.03	20.67	78.01	8.66	186.03	20.67
245	117	31	279	31	279	13

Table 6.20: Real power consumption (three phase major fault scenario)

DER	***Phase a***	***Phase b***	***Phase c***
PV1	331.55	938.87	439.57
PV2	1262.47	59.7	1080.83
PV3	861.03	915.01	699.03
PV4	9.3	164.67	22.5

Table 6.21: Reactive power consumption (three phase major fault scenario)

DER	***Phase a***	***Phase b***	***Phase c***
PV1	50.64	117.95	21.23
PV2	146.32	3.03	117.64
PV3	113.67	65.66	95.67
PV4	1.03	17.86	3.1

distribution network.

6.4 Comparison of Results

In this section, we show the comparison of the results for the linearized single phase and three phase MILP formulations for the different scenarios considered above. We compare the number of iterations, solver times and the percentage of the outage region being supplied by the DERs for all the scenarios. The number of iterations for both formulations in all the scenarios are summarized in Table 6.22. As it can be seen from Table 6.22, the number of iterations increase exponentially with the size of the problem. The number of iterations of the three-phase MILP problem is higher than that of the single phase formulation for the each of the scenario. When we consider the major fault scenario in three phases, in which the entire network experiences power outage, the problem size increases significantly and in turn, the number of iterations required to find an optimal solution increases.

Next, we compare the solution time of each of the scenarios for both problems in in Table 6.23. As displayed in the table, the solution time of for most of the

Table 6.22: Comparison of number of iterations

Iterations	**Single Phase**		**Three Phase**			
			Mixed Phase		**Three Phase**	
	Multiple Faults	**Major Fault**	**Multiple Fault**	**Major Fault**	**Multiple Fault**	**Major Fault**
MIP Simplex Iteration	145	1133	999	46507	719	962,984
Branch-and-Bound Nodes	0	0	0	268	0	2923

Table 6.23: Comparison of solution time

Time (seconds)	**Single Phase**		**Three Phase**			
			Mixed Phase		**Three Phase**	
	Multiple Faults	**Major Fault**	**Multiple Fault**	**Major Fault**	**Multiple Fault**	**Major Fault**
Input	0.000999	0.002999	0.001998	0.004998	0.001999	0.001
Solve	0.047992	1.07484	0.26296	26.62	0.239963	435.64
Output	0	0	0.001	0.001	0.001	0.004999

scenarios considered for the single and three phase MILP problem are less than 2.5 seconds. Only in the major fault scenario for the three phase problem, the time becomes significantly higher due to its problem size. The maximum solver time is 435 seconds for the major fault scenario when DERs are connected in all three phases in the network. Though this solution time is significantly higher than others, it is acceptable considering the size of problem being solved. The bar chart in Figure 6.5 shows the comparison for the solver time for different scenarios.

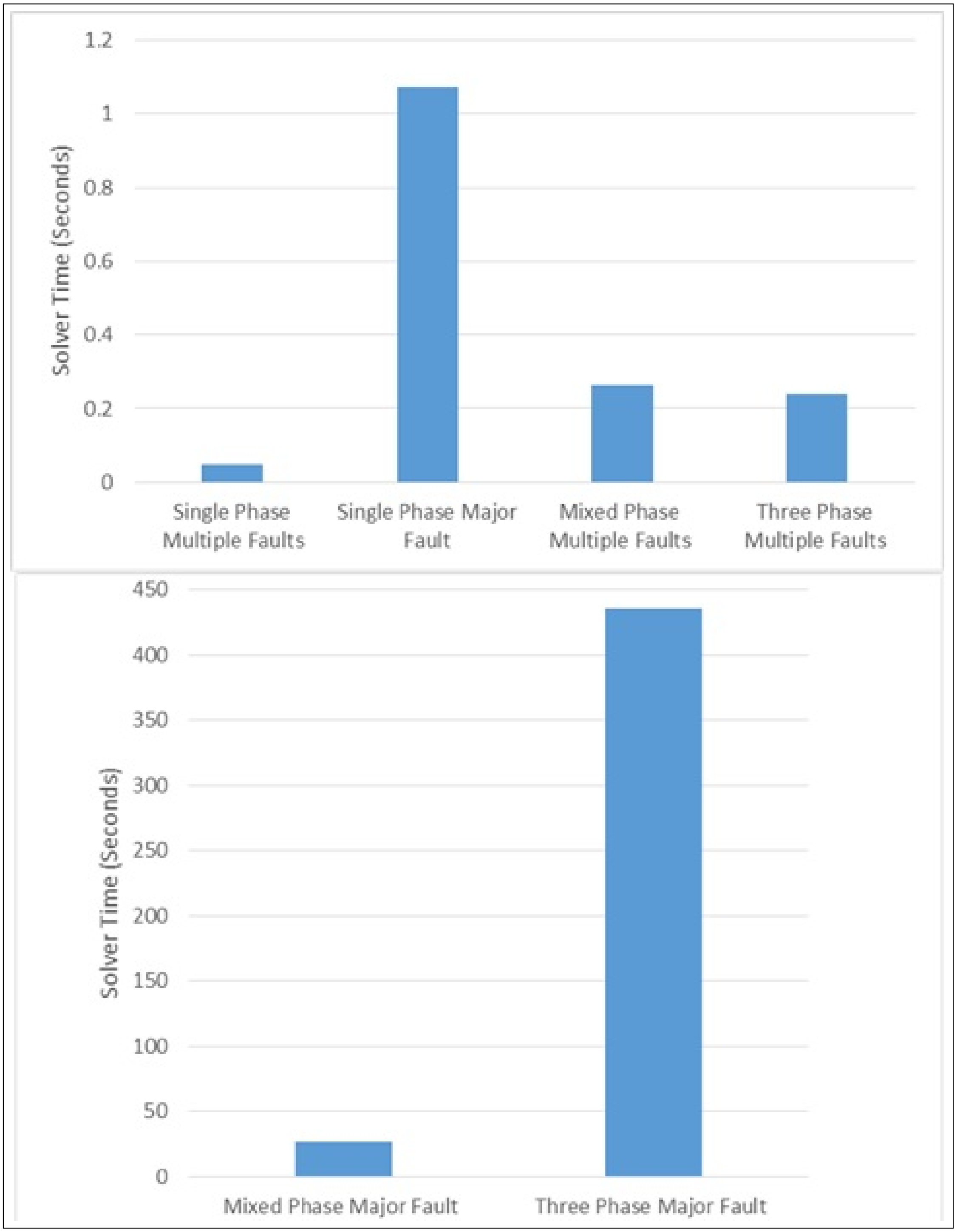

Figure 6.5: Bar chart comparison for solution time

We also present a comparison of the percentage of DER power penetration in the distribution network. For the multiple faults and major fault scenarios, the total load under faulty region is 10524.06 KVA and 16763.04 KVA, respectively. Therefore, the

Table 6.24: Comparison of DER penetration in outage area

Scenario		Penetration allowed by DER	Demand satisfied by DER	DER capacity utilized
Multiple Faults	**Single Phase**	64.65%	55.40%	85.72%
	Mixed Phase		44.50%	65.52%
	Three Phase		55.40%	89.69%
Major Fault	**Single Phase**	40.59%	38.50%	94.85%
	Mixed Phase		39.50%	97.49%
	Three Phase		40.47%	99.71%

percentage of load under faulty region is 64% and 100% respectively. Recall that, the total power capacity for the DERs was set as 40.59% of the total power required in the distribution system i.e. 40.59% of 16763.04 KVA. For the multiple faults scenario, 10524.06 KVA is in the faulted regions, the DERs can supply up to 64.65% of the demand. In the major fault scenario, the total load demand is 16763.04 KVA in the faulty region, hence the DER can only satisfy 40.59% of the demand. The percentage of penetration level for the both the scenarios and the percentage of DER capacity utilized are summarized in the table 6.24 below.

As seen from the table above, the total DER penetration is lowest for the in scenario of the mixed phase with multiple faults in system. This is because the system configuration limits the use of DERs connected only in a single phase. That is, the two single phase DERs considered were not able to supply much power due the network topology constraints. If other locations of DERs were considered, the single phase DERs may be able to supply more power based on the network topology. Overall, for the single phase, the DERs penetrate a relatively large percentage of the load demand. However, the highest load demand and maximum number of high priority loads are satisfied in both scenarios when the DERs are connected in all the three phases. Since, the three phase model provides a better network representation than the single phase model, the three phase model can be used effectively to dynamically form of micro-grids with multiple faults in the distribution system.

CHAPTER 7: CONCLUSION AND FUTURE SCOPE

With the increasing number of outages outages caused by inclement weather, there is a great potential that DERs can utilized to provide electricity to the customers when conventional power source is unavailable due to faults. The aim of this thesis was to introduce optimization models to utilize the distributed energy resources in our distribution network to enhance its resiliency. Beginning with a single phase distribution network, we propose a series of MIP formulations that progressively accomodate more realistic systems. The development of models was conducted in two directions, one by incorporating three phase distribution network, and the other by embracing nonlinear power balance equations. However, we observed that, although the nonlinear formulation can be used to solve the small network example considered quickly became computationally intractable as the problem size increases. Non-radial or meshed network are quite common in real systems. For non-radial network, we propose a method that converts non-radial network to radial network using the shortest path algorithm. Once, converted to radial network, it can be formulated as the proposed model.

The work presented in this thesis can serve as a platform to dive into advanced topics and methods to be utilized in enhancing the grid resiliency. For instance, the optimization model for three phase network can be extended by adopting to nonlinear power balance constraints as done for the single phase model. The proposed models do not consider switching and recloser operations within the network, and can be added as additional constraints in the formulation to enhance the models. We consider only a single source per micro-grid, the effects of multiple sources in a micro-grid should also be studied. There is potential for modify the proposed models to incorporate the

DERs and interconnections between adjoining distribution network and their switching behavior to better capture the actual working with multiple faults in the grid during extreme weather events.

BIBLIOGRAPHY

[1] Design for distributed energy resources Driesen, Johan and Katiraei, Farid Power and Energy Magazine, IEEE volume 6 pages 30–40 year 2008

[2] Only connect: Microgrids for distribution system restoration Che, Liang and Khodayar, Mohammad and Shahidehpour, Mohammad Power and Energy Magazine, IEEE volume 12 pages 70–81 year 2014

[3] Walmart Now Produces More Solar Power Than 38 U.S. States Hower, M. 2013, October 30 Accessed April 07, 2016 http://www.sustainablebrands.com/news_and_views/clean_tech/mike-hower/walmart-now-produces-more-solar-power-38-us-states

[4] The future of Distribution System Resiliency Davis, Glenn and Snyder, Aaron F and Mader, James Power Systems Conference (PSC), 2014 Clemson University pages 1–8 year 2014

[5] Weather-related power outages and electric system resiliency Campbell, Richard J year 2012 Congressional Research Service, Library of Congress

[6] Planning with MIP for Supply Restoration in Power Distribution Systems Thiébaux, Sylvie and Coffrin, Carleton and Hijazi, Hassan L and Slaney, John K and others IJCAI year 2013

[7] An expert system operational aid for restoration and loss reduction of distribution systems Liu, Chen-Ching and Lee, Seung Jae and Venkata, SS Power Systems, IEEE Transactions on volume 3 pages 619–626 year 1988

[8] A rule-based expert system with colored Petri net models for distribution system service restoration Chen, Chao-Shun and Lin, Chia-Hung and Tsai, Hung-Ying Power Systems, IEEE Transactions on volume 17 pages 1073–1080 year 2002

[9] Service restoration of primary distribution systems based on fuzzy evaluation of multi-criteria Lee, Seung-Jae and Lim, Seong-II and Ahn, Bok-Shin Power Systems, IEEE Transactions on volume 13 pages 1156–1163 year 1998

[10] Service restoration methodology for multiple fault case in distribution systems Lim, Seong-Il and Lee, Seung-Jae and Choi, Myeon-Song and Lim, Dong-Jin and Ha, Bok-Nam Power Systems, IEEE Transactions on volume 21 pages 1638–1644 year 2006

[11] A multi-agent solution to distribution systems restoration Solanki, Jignesh M and Khushalani, Sarika and Schulz, Noel N Power Systems, IEEE Transactions on volume 22 pages 1026–1034 year 2007

[12] Heuristic search approach to distribution system restoration Morelato, AL and Monticelli, A Power Delivery, IEEE Transactions on volume 4 pages 2235–2241 year 1989

[13] Optimized Restoration of Unbalanced Distribution Systems Khushalani, Sarika and Solanki, Jignesh M and Schulz, Noel N Power Systems, IEEE Transactions on volume 22 pages 624–630 year 2007

[14] Distribution system service restoration using the artificial neural network approach and pattern recognition method Hsu, Y-Y and Huang, H-M Generation, Transmission and Distribution, IEE Proceedings volume 142 pages 251–256 year 1995

[15] Multiobjective, multiconstraint service restoration of electric power distribution system with priority customers Kumar, Yogendra and Das, Biswarup and Sharma, Jaydev Power Delivery, IEEE Transactions on volume 23 pages 261–270 year 2008

[16] An AIS-ACO hybrid approach for multi-objective distribution system reconfiguration Ahuja, Ashish and Das, Sanjoy and Pahwa, Anil Power Systems, IEEE Transactions on volume 22 pages 1101–1111 year 2007

[17] Agent based restoration with distributed energy storage support in smart grids Nguyen, Cuong P and Flueck, Alexander J Smart Grid, IEEE Transactions on volume 3 pages 1029–1038 year 2012

[18] Analyzing the reliability impact of distributed generation Brown, Richard E and Freeman, Lavelle AA Power Engineering Society Summer Meeting, 2001 volume 2 pages 1013–1018 year 2001

[19] Resilient Distribution System by Microgrids Formation After Natural Disasters Chen, Chen and Wang, Jianhui and Qiu, Feng and Zhao, Dongbo IEEE

[20] New challenges in power system restoration with large scale of dispersed generation insertion Pham, Thi Thu Ha and Bésanger, Yvon and Hadjsaid, Nouredine Power Systems, IEEE Transactions on volume 24 pages 398–406 year 2009

[21] Novel multiagent based load restoration algorithm for microgrids Xu, Yinliang and Liu, Wenxin Smart Grid, IEEE Transactions on volume 2 pages 152–161 year 2011

[22] Microgrid provision of blackstart in disaster recovery for power system restoration Castillo, Alejandro Smart Grid Communications (SmartGridComm), 2013 IEEE International Conference on pages 534–539 year 2013

[23] Distribution system restoration with microgrids using spanning tree search Li, Juan and Ma, Xi-Yuan and Liu, Chen-Ching and Schneider, Kevin P Power Systems, IEEE Transactions on volume 29 pages 3021–3029 year 2014

[24] Microgrid Restoration after Major Faults in Main Grid with Automatic and Constant Time Switching Zare, Elyas and Shahabi, Majid International Journal of Intelligent Systems and Applications volume 5 pages 50 year 2013

[25] Self-healing resilient distribution systems based on sectionalization into microgrids Wang, Zhaoyu and Wang, Jianhui Power Systems, IEEE Transactions on volume 30 pages 3139–3149 year 2015

[26] A brief history of linear and mixed-integer programming computation Bixby, Robert E Documenta Mathematica pages 107–121 year 2012

[27] How companies use optimization IBM Accessed April 14, 2016 `https://www-01.ibm.com/software/websphere/optimization/benefits/`

[28] Applied mathematical programming Bradley, Stephen and Hax, Arnoldo and Magnanti, Thomas year 1977 publisher Addison Wesley

[29] Optimal capacitor placement on radial distribution systems Baran, Mesut E and Wu, Felix F Power Delivery, IEEE Transactions on volume 4 pages 725–734 year 1989

[30] Adaptive VAR control for distribution circuits with photovoltaic generators Yeh, Hen-Geul and Gayme, Dennice F and Low, Steven H Power Systems, IEEE Transactions on volume 27 pages 1656–1663 year 2012

[31] Methods of nonlinear 0-1 programming Hansen, Pierre Annals of Discrete Mathematics volume 5 pages 53–70 year 1979

[32] Investigation of Model Techniques–First Annual Report–6 June 1956–1 July 1957–A Study of Model Techniques for Communication Systems Leyzorek, M and Gray, RS and Johnson, AA and Ladew, WC and Meaker Jr, SR and Petry, RM and Seitz, RN Case Institute of Technology, Cleveland, Ohio year 1957

[33] AMPL: A mathematical programming language Fourer, Robert and Gay, David M and Kernighan, Brian W year 1987 publisher AT&T Bell Laboratories Murray Hill, NJ 07974

[34] CPLEX v12. 1 ILOG, IBM Users Manual for CPLEX year 2009

[35] NEOS Server 4.0 administrative guide Dolan, Elizabeth D arXiv preprint cs/0107034 year 2001

[36] The NEOS server for optimization: Version 4 and beyond Dolan, E and Fourer, Robert and Moré, Jorge J and Munson, Munson and others Preprint ANL/MCS-TM-253, Mathematics and Computer Science Division, Argonne National Laboratory year 2002

[37] The Kestrel Interface to the NEOS Server1 Dolan, Elizabeth D and Munson, Todd S year 2001

[38] Optimization on the NEOS server Dolan, Elizabeth D and Fourer, Robert and Moré, Jorge J and Munson, Todd S SIAM News volume 35 page 4 year 2002

[39] BARON: A general purpose global optimization software package author Sahinidis, Nikolaos V Journal of global optimization volume 8 pages 201–205 year 1996